

# Dihydrofolate reductase: structural aspects of mechanisms of enzyme catalysis and inhibition

V. I. Polshakov

Center for Drug Chemistry, All-Russian Chemical and Pharmaceutical Research Institute,  
7 Zubovskaya ul., 119815 Moscow, Russian Federation.  
Fax: +7 (095) 246 7805. E-mail: polsha@drug.org.ru

The mechanism of catalytic reduction of folic and dihydrofolic acids to tetrahydrofolate, which proceeds under the action of dihydrofolate reductase and the coenzyme NADPH, is considered. The roles of the enzyme active site, the coenzyme, individual amino acid residues of the enzyme, and water molecules in the catalytic reaction are discussed. Interactions of the enzyme with competitive inhibitors many of which are widely used in medicine as antitumor and antibacterial drugs are examined. The factors controlling the selectivity of inhibitor binding to bacterial forms of the enzyme are analyzed. The results of X-ray diffraction and NMR spectroscopic studies of the structures of the enzyme and its complexes with the substrate and inhibitors are surveyed. The role of specific interactions and molecular motions of the protein and ligands in the mechanism of catalysis and in the binding of the ligands to the enzyme is discussed.

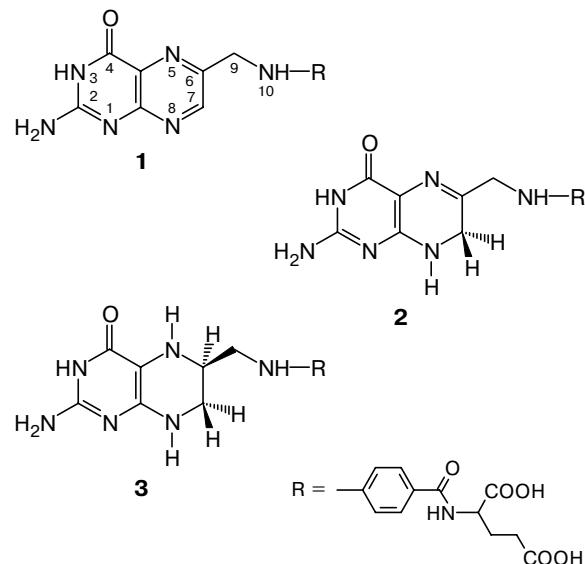
**Key words:** dihydrofolate reductase, mechanism of enzyme catalysis, protein–ligand binding, protein structure, X-ray diffraction analysis, NMR spectroscopy, mechanism of functioning of antifolate drugs.

## 1. Introduction

In recent years, processes of molecular recognition have attracted considerable attention of researchers engaged in medical chemistry. This interest was stimulated primarily due to qualitative changes in this field of chemistry. Thus in the search for new drugs, researchers turned from the strategy of the total screening to rational methods based on a knowledge of the structure of a potential biological target. These approaches are based both on a knowledge of the three-dimensional structure of the target of action of the drug and an understanding of the nature of the highly specific ligand binding to the biomolecule. Considerable progress in this field has been achieved due to investigations of the enzyme dihydrofolate reductase and its interactions with antifolate drugs. These studies provided abundant valuable data, which can be used in the examination of the ligand binding to many other proteins, which are potential targets of action of various pharmaceuticals.

Dihydrofolate reductase (DHFR) catalyzes reduction of folic (Fol, **1**) and dihydrofolic ( $\text{H}_2\text{Fol}$ , **2**) acids to tetrahydrofolic acid ( $\text{H}_4\text{Fol}$ , **3**).<sup>1</sup> Since tetrahydrofolate and its metabolites are involved in the biosynthesis of thymidine monophosphate (dTMP), purine bases, and methionine (Fig. 1), it is necessary to maintain a rather high concentration of pool **3** for normal vital activity of the cell.

Blocking of the enzyme functioning causes termination of cell division and subsequent cell death. This



phenomenon serves as the basis for functioning of inhibitors of dihydrofolate reductase, *viz.*, the so-called antifolate drugs many of which are widely used in medicine for the treatment of tumor diseases (Methotrexate (MTX, **4**) and Trimethrexate (TMQ, **5**)), bacterial infections (Trimethoprim (TMP, **6**)), and protozoan infections (Pyrimethamine, (PMX, **7**)). These drugs compete with dihydrofolate **2** for the substrate binding site in DHFR and their therapeutic properties depend significantly on the strength and selectivity of

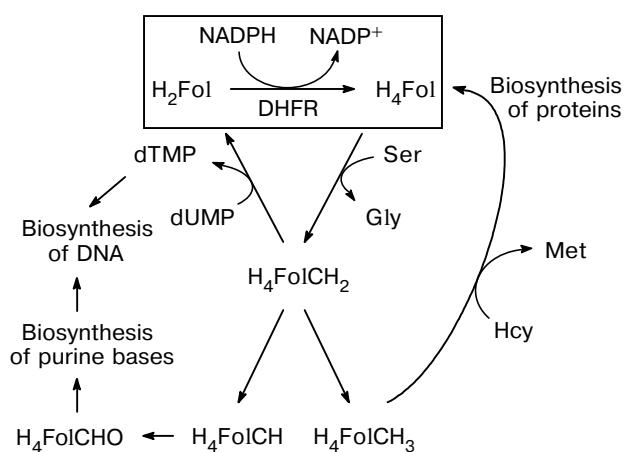
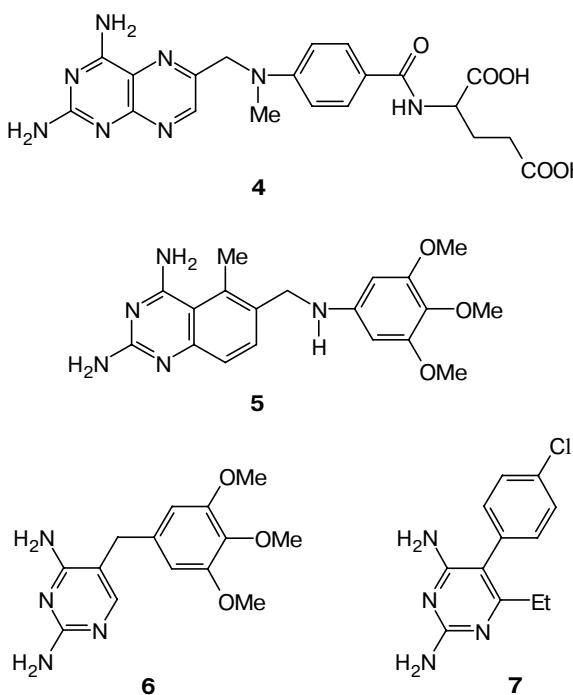


**Fig. 1.** Dihydrofolate reductase in metabolism of derivatives of folic acid and their role in the biosynthesis of nucleic acids and proteins.

binding of inhibitors to the enzyme of pathogenic cells. For example, the binding of drug **6** to bacterial forms of DHFR is several thousand times stronger than the binding to the human enzyme (see Section 4.3) due to which the drug exhibits high antibacterial activity.



In 1988, Hitchings, Elion, and Black were honored with the Nobel prize in Physiology and Medicine for the discovery of the selective binding of **6** and some other pharmaceuticals to targets.<sup>2</sup> However, the molecular nature of this selectivity is still not completely understood.<sup>3</sup>

The present review does not give an exhaustive survey of all problems concerning the mechanisms of functioning and inhibition of DHFR. From one to two

hundred research articles devoted to these problems were published in the literature every year. Some of these studies were concerned with the fundamental aspects of the mechanism of DHFR catalysis and interactions of the enzyme with various ligands, but most of these studies, in one way or another, were associated with the search for new biologically active compounds in the series of DHFR inhibitors. In spite of the fact that DHFR is among the most thoroughly and comprehensively studied enzymes, many fundamental problems of the mechanism of functioning of DHFR and the nature of specific interactions with inhibitors remain to be solved. At the same time, investigations of this enzyme as well as ideas and methods aimed at solving the related problems have many applications in molecular biology and pharmacology. The present review surveys primarily the structural aspects of the mechanism of DHFR catalysis and interactions of the enzyme with its inhibitors.

## 2. Structures of complexes of dihydrofolate reductase

The structures of bacterial forms of the enzyme and DHFR species from high organisms were established by X-ray diffraction analysis and NMR spectroscopy. Early in 2000, the Brookhaven Protein Databank contained 83 structures of DHFR from *Escherichia coli*,<sup>4–12</sup> *Lactobacillus casei*,<sup>4,13–16</sup> *Pneumocystis carinii*,<sup>17–20</sup> *Mycobacterium tuberculosis*,<sup>21</sup> *Thermotoga maritima*,<sup>22</sup> *Candida albicans*,<sup>23</sup> and *Haloflexax volcanii*,<sup>24</sup> human DHFR,<sup>18,25–29</sup> and the chicken pancreatic enzyme.<sup>30–32</sup> First high-resolution structures of the DHFR complexes in solution were established for the enzyme from *Lactobacillus casei*.<sup>15,16</sup> The more detailed data on the known structures of DHFR are given in Table 1.

Dihydrofolate reductase is a relatively small water-soluble protein (with the molecular weight of 18000–25000 Da for most of the enzyme species isolated from various sources). The enzyme consists of eight  $\beta$ -sheets, which compose a rather rigid skeleton of the protein molecule (Fig. 2). All forms of the enzyme contain at least four  $\alpha$ -helices one of which makes up the substrate binding site and two other helices compose the coenzyme binding site (Fig. 3). The enzyme contains no disulfide bonds, and coordination of the metal ions is not necessary for the manifestation of its biochemical activity.

The protein contains several structural elements common to all enzyme forms. Among these elements are the loop I located between the  $\beta$ -sheet **a** and the  $\alpha$ -helix B and the *cis*-peptide bond between two glycine residues located at the junction of the  $\beta$ -sheet **e** and the  $\alpha$ -helix F (G98 and G99 in the *L. casei* enzyme). The amino acid sequence alignment for DHFR from different organisms (Fig. 4) revealed a series of strictly conserved residues most of which play an important role in the mechanism of catalysis. Virtually all these residues are

**Table 1.** Structures of the DHFR complexes with substrates, coenzymes, and inhibitors

Source of the enzyme	Ligand	PDB code	Reso- lution /Å	Ref- erence	Source of the enzyme	Ligand	PDB code	Reso- lution /Å	Ref- erence
<i>Escherichia coli</i>	Fol	1rd7	2.60		<i>Lactobacillus casei</i>	MTX, NADPH	3dfr	1.70	4
		1rx7	2.30	11		MTX	1ao8	NMR	15
	Fol	1dyi	1.90	9		TMQ	1bfz	NMR	16
	DZF <sup>a</sup>	1dyh	1.90	9		Brodimoprim- 4,6-dicarboxylate	1dis	NMR	14
	H <sub>2</sub> Fol	1rf7	1.80	11	<i>Pneumocystis carinii</i>	Fol	1diu		
	DDF <sup>b</sup>	1dyj	1.85	9		Fol, NADP <sup>+</sup>	4cd2	2.00	19
	DDF	1rx5	2.30	11		Fol, NADP <sup>+</sup>	2cd2	1.90	19
	Leucovorin	1jol	1.96			TAB, <sup>c</sup> NADPH	1cd2	2.20	19
		1jom	1.90	10		COE, <sup>d</sup> NADPH	1d8r	2.10	20
	NADPH	1ra1	1.90			TMP, NADPH	1daj	2.30	18
		1rx1	2.40	11		MTX, NADP <sup>+</sup>	1djr	1.86	17
	NADP <sup>+</sup>	1ra9	1.55			MTX, NADP <sup>+</sup>	3cd2	2.50	19
		1rx9	1.90	11	<i>Mycobacterium tuberculosis</i>	MTX, NADP <sup>+</sup>	1df7	1.70	21
	NADP <sup>+</sup>	1drh	2.30	9		TMP, NADP <sup>+</sup>	1dg5	2.00	21
	Fol, NADP <sup>+</sup>	1ra2	1.60			WRB, NADP <sup>+</sup>	1dg7	1.80	21
		1rb2	1.60	11		NADP <sup>+</sup>	1dg8	2.00	21
		1rx2	1.80			NADPH, MTX	1d1g	2.10	22
	Fol, ATR	1ra8	1.80	11		—	1cz3	2.10	22
	DDF, NADP <sup>+</sup>	1rc4	1.90	11		CW345, <sup>e</sup>	1aoe		23
	DDF, AP	1rx4	2.20	11		NADPH	1ai9	1.85	23
	DDF, NADPH	1rx6	2.00	11		NADPH	1vdr	2.55	24
	Fol, AP	1rx8	2.80	11		NADPH	1drf	2.00	25
	MTX	1ddr	2.20	12	<i>Thermotoga taritima</i>	DZF	1dhf	2.30	26
		1dds	2.20			PRD, <sup>f</sup> NADPH	1boz	2.10	29
	MTX	3drc	1.90	7		PT523, NADPH	1ohj	2.50	28
	MTX	4dfr	1.70	4		—	1ohk	2.50	
	MTX	1rg7	2.00	11		MOT, <sup>g</sup> NADPH	1hfr	2.10	18
	MTX, NADPH	1rh3	2.40			MOT, NADPH	1hfp	2.10	18
		1rx3	2.20	11		MOT, NADPH	1hfq	2.10	18
	MTX, NADP <sup>+</sup>	1dre	2.60			Human F31G	1dlr	2.30	27
		1ra3	1.80	11		Human F31S	1dra	2.30	32
		1rb3	2.30			Human L22Y	1drb	2.30	32
<i>Escherichia coli</i> D27S	MTX	1dhi	1.90	8		Human L22F	1dr3	2.30	32
<i>Escherichia coli</i> W22F	MTX	2drc	1.90	7		Chicken Liver	8dfr	1.70	30
<i>Escherichia coli</i> D27S, F137S	MTX	1dhj	1.90	8		NADPH	1dr1	2.20	31
<i>Escherichia coli</i> D27E	MTX	1dra	1.90	6		Biopterin, NADP <sup>+</sup>			
<i>Escherichia coli</i> D27C	MTX	1drb	1.90	6		Thio NADP <sup>+</sup>			
<i>Escherichia coli</i> (TMP-stable)	—	5dfr	2.30	6		Biopterin, Thio NADP <sup>+</sup>			
	NADP <sup>+</sup>	6dfr	2.30	5					
	Fol, NADP <sup>+</sup>	7dfr	2.50	5					

<sup>a</sup> DZF is 5-deazafolate.<sup>b</sup> DDF is 5,10-dideazatetrahydrofolate.<sup>c</sup> TAB is acetyl-*N*-[2-chloro-5-(2,4-diamino-6-ethylpyrimid-5-yl)phenyl][benzyltriazen-3-yl] ethyl ether.<sup>d</sup> COE is furo[2,3-*d*]pyrimidine.<sup>e</sup> CW345 is 1,3-diamino-7-(pent-3-yl)-7*H*-pyrrolo[3,2-*f*]quinazoline.<sup>f</sup> PRD is 2,4-diamino-6-[*N*-(2,5-dimethoxybenzyl)-*N*-methylamino]pyrido[2,3-*d*]pyrimidine.<sup>g</sup> MOT is *N*-[4-{[(2,4-diaminofuro[2,3-*d*]pyrimidin-5-yl)methyl]methylamino}benzoyl] L-glutamate.

involved in the substrate or coenzyme binding sites and their role will be discussed in more detail. Noteworthy also are the rather low homology between different DHFR species (less than 30%)<sup>33</sup> simultaneously with the high structural similarity.

The enzyme active site is located in the hydrophobic pocket surrounded by the α-helix B, the central β-sheets (**a**, **e**, and **b**), and the loop I (see Fig. 3). The pteridine

fragment of the substrate resides virtually in the center of the protein and its *p*-aminobenzoylglutamine residue is involved in a Coulomb contact with the conserved arginine residue (Arg57 in the enzyme from *L. casei*) located almost at the surface. The major portion of the coenzyme molecule (NADP<sup>+</sup>)\* is bound to the protein

\* NADP<sup>+</sup> is nicotinamide adenine dinucleotide phosphate.

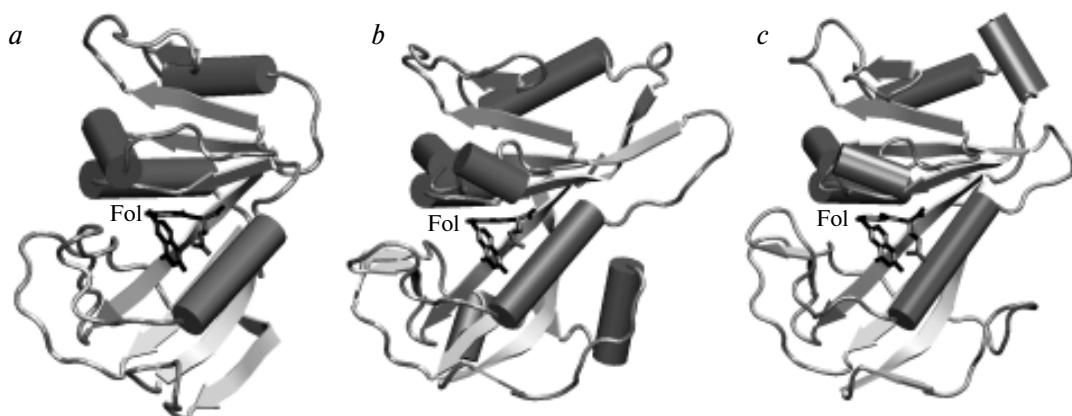


**Fig. 2.** Schematic representation of the binary complexes of three different forms of DHFR with folate (Fol); the  $\alpha$ -helices of the protein are displayed as tubes and the  $\beta$ -sheets are shown as arrows corresponding to the direction of the protein chain: (a) DHFR from *Escherichia coli* (Brookhaven PDB code 1rx7);<sup>11</sup> (b) DHFR from *Pneumocystis carinii* (4cb2);<sup>19</sup> (c) the human enzyme (1drf).<sup>25</sup>

amino acid residues, which are also located at the protein surface; however, the nicotinamide fragment resides in a deep pocket in the vicinity of the substrate. The close arrangement of the C(4) atom of the nicotinamide fragment and the C(6) and C(7) atoms of the substrates facilitates the hydride-ion transfer in the course of the catalytic event.

Methotrexate **4**, which is a classical DHFR inhibitor, was synthesized as a compound structurally similar to the enzyme substrate. Compound **4** has long been thought to be bound to the protein in perfect analogy to

Fol (**1**) or H<sub>2</sub>Fol (**2**). More recently, it was demonstrated<sup>34</sup> that the inhibitor is bound to the enzyme so that it is rotated by  $\sim 180^\circ$  compared to substrates **1** and **2** (Fig. 5). In particular, this fact accounts for the complete absence of reduction of the pteridine ring of the inhibitor and the substantially stronger binding of **4** to the enzyme compared to substrates **1–3**. The interaction between MTX and DHFR is still an example of exceptionally strong interactions between the low-molecular-weight ligand and the protein, the constants of dissociation of the inhibitor from complexes with some enzyme species are about  $10^{-11}$  mol L<sup>-1</sup>.<sup>35</sup> The interactions of MTX and other inhibitors with DHFR will be discussed in more detail in Section 4.

### 3. Mechanism of DHFR catalysis

Dihydrofolate reductase catalyzes the reduction reactions **1**  $\rightarrow$  **2** and **2**  $\rightarrow$  **3** using the coenzyme NADPH\*

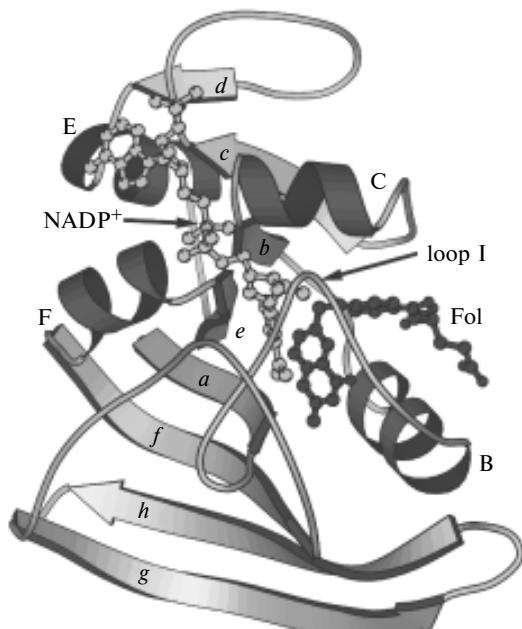
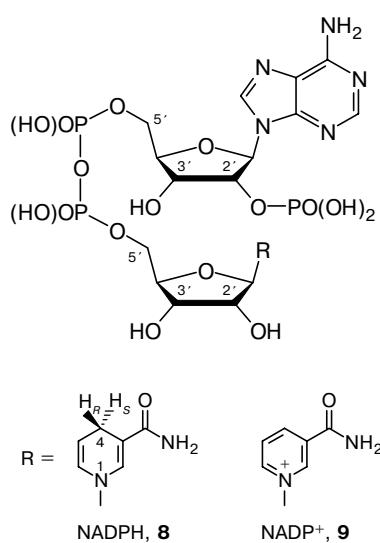


**Fig. 3.** Topology of the protein and the arrangement of the substrate (Fol) and the coenzyme (NADP<sup>+</sup>) in the complex of *Escherichia coli* DHFR. The  $\beta$ -sheets are labeled by lower-case Latin letters (*a*–*g*) and the  $\alpha$ -helices are denoted by capital Latin letters (B, C, E, and F). The atomic coordinates were taken from the X-ray structure of the corresponding ternary complex (Brookhaven PDB code 1rx2).<sup>11</sup>



\* NADPH is the reduced form of dinicotinamide adenine nucleotide phosphate.

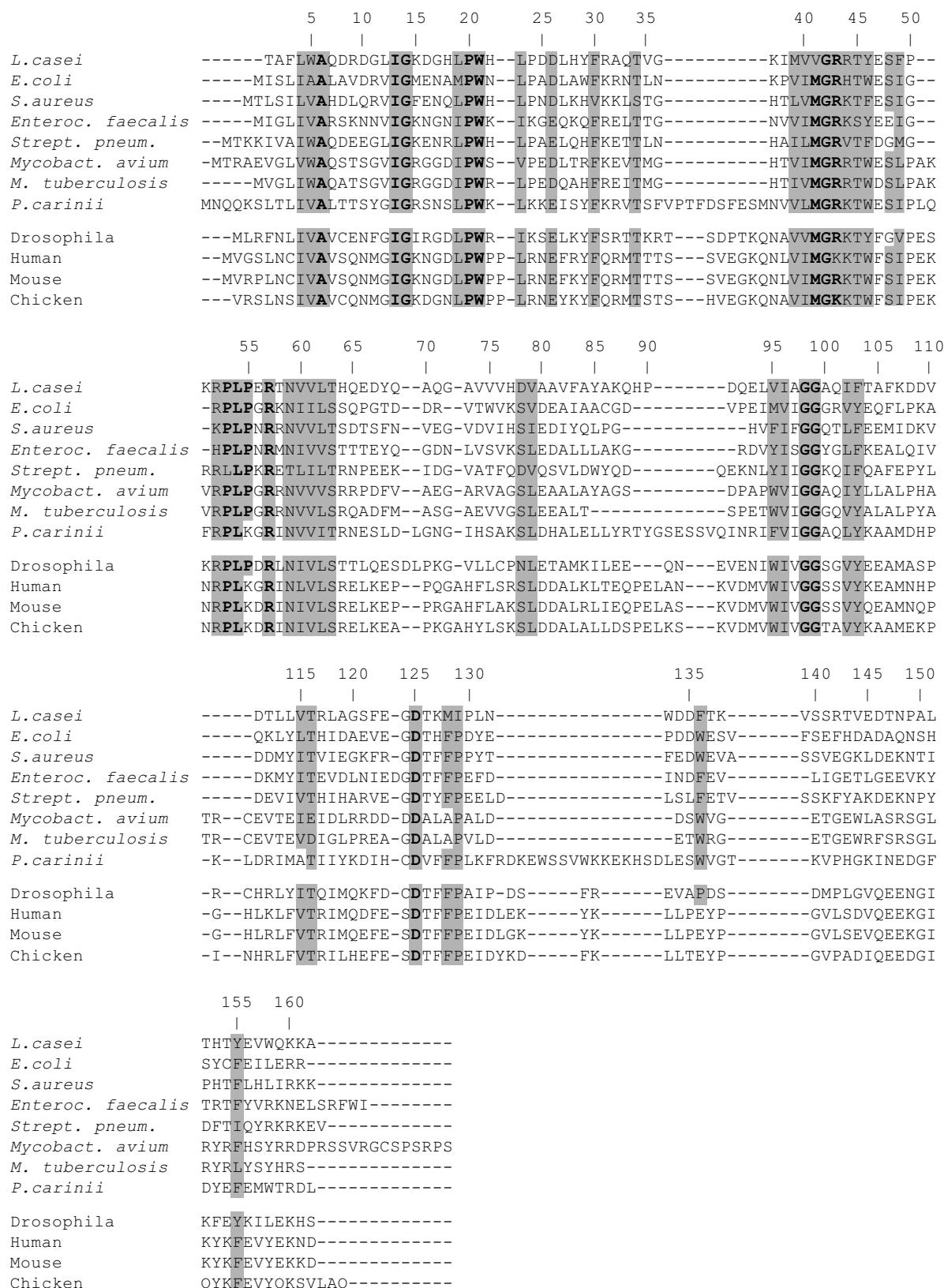


**Fig. 4.** Aligned amino acid sequences of DHFR from prokaryotes (bacteria) and eukaryotes (high organisms). The strictly conserved amino acid residues are given in bold type. The conserved regions are shaded.

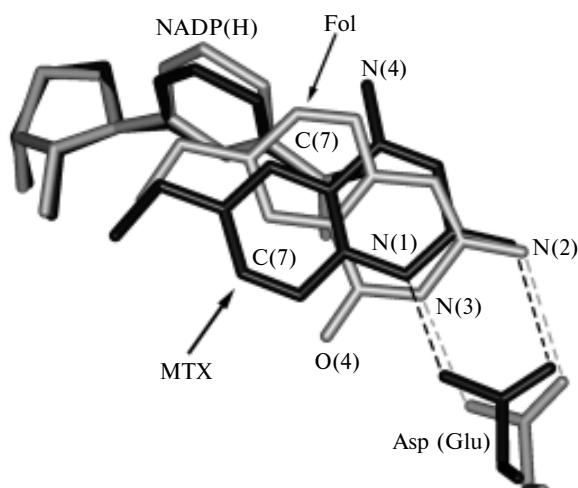


**Fig. 5.** The arrangement of the pteridine ring of MTX (black) and Fol (gray) with respect to the nicotinamide ring of the coenzyme and the carboxy group of the aspartic (glutamic) acid residue. Selected atoms are numbered. The atomic coordinates were taken from the structures of the complexes *E. coli* DHFR-MTX-NADPH (Brookhaven PDB code 1rx3) and *E. coli* DHFR-Fol-NADP<sup>+</sup> (1rx2)<sup>11</sup> and were superimposed by the protein backbones.

and the proton of the water molecule, respectively, as a donor of the hydride ion. The mechanism of DHFR catalysis remains to be the subject of extensive studies. The kinetic and structure aspects of the reaction, the role of individual amino acids in the catalytic reaction, the molecular motions of the enzyme, and the role of molecular motions in the mechanism of catalysis were examined. The key stage, *viz.*, the transfer of the hydride ion from the coenzyme molecule to the substrate, was studied also by quantum-chemical methods with the aim of determining the structure of the transition state and the energy profile of the reaction.

**3.1. Kinetic aspects of reduction of substrates 1 and 2.** The rate of reduction of **2** is approximately two orders of magnitude higher than that of **1**.<sup>36</sup> Since reduction of **2** is the main reaction catalyzed by DHFR in cells, the reaction with this substrate has been studied more extensively. The enzymatic kinetics is an important tool in investigating the mechanism of enzyme catalysis.<sup>37</sup> Extensive kinetic studies were carried out for various DHFR species from *Escherichia coli*,<sup>38–40</sup> *Lactobacillus casei*,<sup>41</sup> and *Pneumocystis carinii*<sup>42</sup> and for mouse<sup>43</sup> and human<sup>44</sup> DHFR. The results of these investigations made it possible to establish the complete scheme of the catalytic reaction **2** → **3**. The rates of association and dissociation of the ligands were measured by the stopped flow method. Among these ligands were the substrate ( $H_2\text{Fol}$ ), the reaction product ( $H_4\text{Fol}$ ), and the reduced and oxidized forms of the coenzyme in the catalytic cycle. The selected results of the investigation carried out for the enzyme from *Escherichia coli*<sup>38</sup> are presented in Fig. 6. In particular, it was established that dissociation of  $H_4\text{Fol}$  is the rate-determining stage

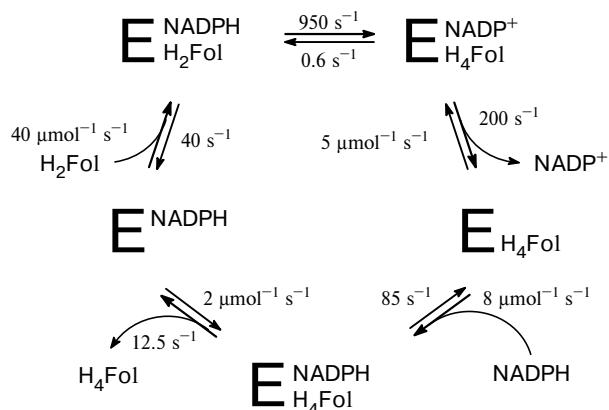


**Fig. 6.** The simplified pH-independent kinetic scheme of the catalytic cycle of DHFR (denoted by E). The rates of association and dissociation of the ligands and the rate of the hydride-ion transfer at 25 °C are given for *Escherichia coli* DHFR.<sup>38</sup>

of the catalytic cycle for all forms of DHFR, the reaction proceeding only once  $\text{NADP}^+$  is replaced by  $\text{NADPH}$ . The reason is that  $H_4\text{Fol}$  and  $\text{NADPH}$  exhibit an essential negative cooperative effect upon the formation of the ternary complex with the enzyme due to which the reaction product leaves the active site more readily. Thus, the constants of binding of  $H_4\text{Fol}$  to *L. casei* DHFR in the presence of  $\text{NADP}^+$  and  $\text{NADPH}$  are decreased by a factor of 3 and 600, respectively.<sup>45</sup> The similar values were observed for the enzyme from *E. coli* (Table 2).

For all studied enzyme species, the rate of transfer of the hydride ion from the coenzyme to the substrate, which is the key stage of the catalytic process, is one of the most rapid stages in the catalytic cycle. Hence, association and dissociation of the ligands are of primary importance in the mechanism of DHFR catalysis and these processes determine the overall rate of the catalytic process. The rates of association and dissociation of the ligands, in turn, are dictated to a great extent by the positive and negative cooperative effects whose molecular nature calls for further investigation.

### 3.2. Stereochemistry of the hydride-ion transfer.

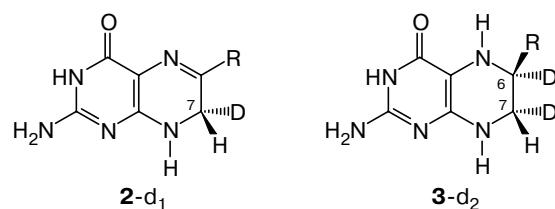
Important information on the mechanism of DHFR catalysis was obtained in the study of the stereochemistry of the hydride-ion transfer. It was found that reduction of 7,8-dihydrofolate (**2**) was accompanied by the transfer of the hydrogen atom located in the 4-*pro-R*

**Table 2.** Cooperativity in the binding ( $K_{\text{coop}}^*$ ) of the pteridine ligands and the coenzyme to *E. coli* DHFR

Coenzyme	$H_2\text{Fol}$	$H_4\text{Fol}$	MTX
NADPH	0.5	0.01	680
NADP <sup>+</sup>	2.4	0.6	12.5

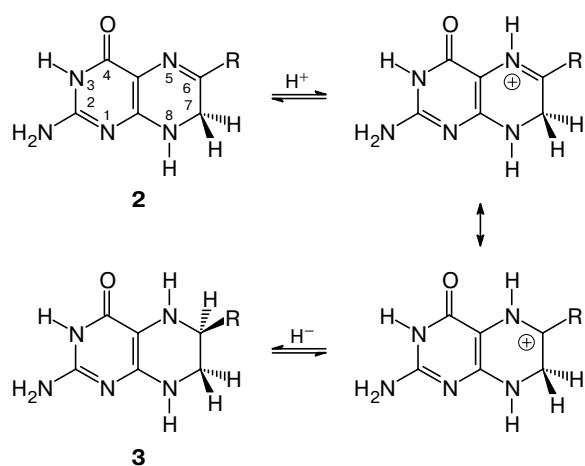
\*  $K_{\text{coop}}$  were calculated as the ratios of the binding constants of the ligand in the ternary complex to the corresponding binding constants in the binary complex.<sup>6,45</sup>

position of NADPH (**8**) to the C(6) atom of dihydrofolate (**2**).<sup>46</sup> The use of the nicotinamide coenzyme, which was selectively labeled with deuterium at the 4-*pro-R* position of the dihydropteridine ring, made it possible to find<sup>47</sup> that reduction of **1** afforded dihydrofolate-d<sub>1</sub> containing the deuterium atom in the 7*S* position (**2-d<sub>1</sub>**). The latter compound was subsequently converted into tetrahydrofolate-d<sub>2</sub>, which possessed the deuterium atoms located on the same side of the dihydropteridine ring (**3-d<sub>2</sub>**). These data have provided unambiguous evidence for the mutual arrangement of the nicotinamide ring of NADPH and the pteridine ring of the substrate within the enzyme active site. More recently, these results were confirmed by X-ray diffraction studies.



**3.3. The mechanism of substrate protonation.** Two factors facilitate the hydride-ion transfer, which is accompanied by a change in the hybridization of the atoms of the nicotinamide ring: the favorable arrangement of the interacting fragments of the substrate and the coenzyme within the active site and the catalytic participation of the amino acid residues surrounding the ligands. The key stage of the catalytic process involves two main steps, *viz.*, protonation of substrate **2** at the N(5) atom and the transfer of the hydride ion to the positively charged intermediate to form neutral reaction product **3** (Scheme 1).

Scheme 1

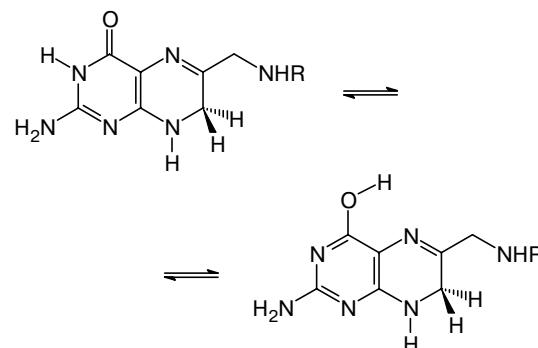


The effect of the replacements of the conserved amino acid residues of DHFR involved in the substrate binding site on the catalytic properties of the enzyme was examined. It was found that the replacement of the

carboxy-containing residue, which is responsible for substrate protonation and generation of the Coulomb interaction with the substrate (Asp26 in the enzyme from *L. casei*, Asp27 in the *E. coli* enzyme, Glu30 in human DHFR, *etc.*), leads to a substantial decrease in the catalytic activity.<sup>48</sup> It was assumed that this amino acid residue is involved in the proton transfer to the substrate.<sup>49</sup> For the enzymatic reaction to proceed, dihydrofolate must be protonated at the N(5) atom of the pteridine residue of **2** or at the N(8) atom in the reduction of folate **1**.<sup>1</sup> In this case, the transfer of the hydride ion from the coenzyme proceeds readily. At the same time,  $pK_a$  of free dihydrofolate (**2**) upon its protonation at the N(5) atom is 2.6,<sup>50</sup> *i.e.*, the substrate at physiological pH is protonated to only a small extent. However, the pH dependence of the rate of the hydride-ion transfer indicates that  $pK_a$  of the substrate (for N(5)) in its complex with the enzyme is 6.5.<sup>38</sup> Therefore, the mechanism of catalysis depends substantially on the ability of the enzyme to raise  $pK_a$  of the substrate by almost four units. The main amino acid residue involved in this process is the residue of aspartic (Asp26 in the enzyme from *L. casei*; Asp27 in the enzyme from *E. coli*) or glutamic acid (Glu30 in human DHFR). This assumption is strongly supported by the fact that the above-mentioned residue is the only ionizable amino acid residue located in the active site of the enzymes from all sources.<sup>13,19,25</sup> In addition, the replacement Asp27 (*E. coli*) → Ser leads to a decrease in the rate of reduction of the substrate and to a sharp shift of the maximum of the catalytic activity of the enzyme to low pH,<sup>49</sup> which is indicative of the involvement of this residue in substrate protonation.

It is known that free substrate **2** can exist both in the keto and tautomeric enol forms<sup>51</sup> (Scheme 2).

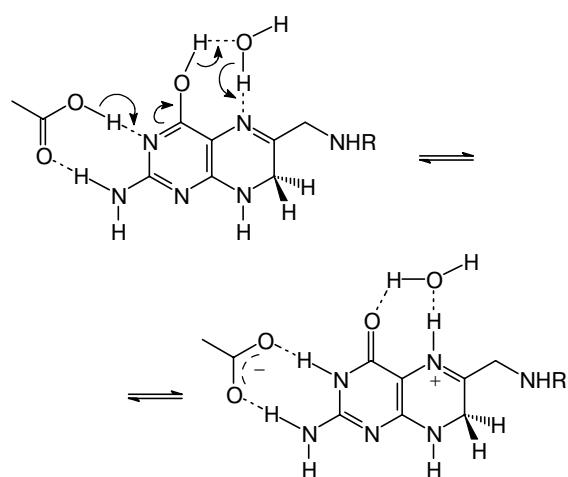
Scheme 2



Analysis of the NMR<sup>52,53</sup> and Raman<sup>54</sup> spectra demonstrated that the keto form is the major tautomeric form of the substrate in its complex with DHFR. Binding of the enol form of the substrate to the enzyme gives rise to a complex adopting an inactive conformation (similar to that in the case of the complex with MTX; see Fig. 5) in which reduction does not occur.<sup>55,56</sup>

Nevertheless, the equilibrium between two tautomeric forms is also possible for the substrate bound to the enzyme. In the latter case, it was assumed that the interaction of the enol form with the carboxy group of the aspartic (glutamic) acid residue can play the key role in the mechanism of protonation of substrate **2** at the N(5) atom *via* the proton transfer through a water molecule<sup>5,57</sup> (Scheme 3).

Scheme 3



This process has been examined thoroughly by several research groups using various experimental techniques. However, a number of problems remain to be solved. Thus, Raman spectroscopic studies demonstrated that the binary complex DHFR—H<sub>2</sub>Fol contains the substrate in the nonprotonated form, and protonated dihydrofolate was detected only on going to the ternary

complex DHFR—H<sub>2</sub>Fol—NADPH.<sup>54</sup> The NMR studies of the binary complexes of <sup>13</sup>C- and <sup>15</sup>N-labeled folic acid **1** with human DHFR showed that the N(3) atom in **1** exists in the amino form even at pH 9.5.<sup>52</sup> Hence, the substrate involved in the complex at physiological pH exists virtually exclusively in the keto(amino) form. It was concluded that the schemes of protonation at the N(5) atom involving the enol form are incorrect. The fact that pK<sub>a</sub> of the carboxy group of the residue Asp27 (in the *E. coli* enzyme) is lower than 5.0<sup>58</sup> and, consequently, it cannot govern the enzymatic reaction is rather unexpected (recall that pK<sub>a</sub> for substrate **2** in the complex with the enzyme is ~6.5). Analogous conclusions were made based on the examination of the NMR spectra of the complexes of <sup>13</sup>C—H<sub>2</sub>Fol and <sup>15</sup>N—H<sub>2</sub>Fol with human DHFR.<sup>52</sup> The ionization state of the residue Glu30 in human DHFR was measured in the pH range from 5 to 7. Based on the results obtained, it was concluded that ionization of this amino acid residue cannot be responsible for the observed pH dependence of the rate of proton transfer. Analogous results were obtained for the residue Asp26 in *L. casei* DHFR.<sup>59</sup> The authors of the cited investigations suggested that the pH dependence of the rate of the catalytic reaction is primarily determined by the contributions of amino acid residues remote from the enzyme active site as well as by the contributions of the coenzyme and water molecules.

Actually, X-ray diffraction studies revealed several long-lived water molecules coordinated in the vicinity of the substrate or the inhibitor (Fig. 7) in complexes with all studied forms of the enzyme. For example, two water molecules, *viz.*, Wat 253 and Wat 201, were found in the complex of *L. casei* DHFR with MTX and NADPH.<sup>4</sup> Analogous molecules (O 237 and O 247)

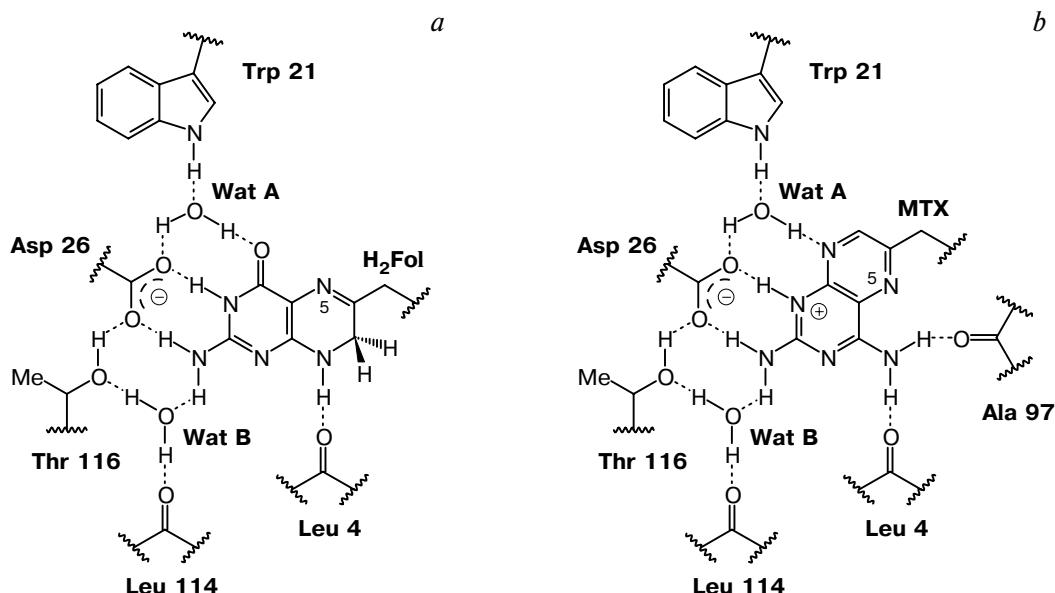


**Fig. 7.** Arrangement of the water molecules Wat A (253) and Wat B (201) in the X-ray structure of the complex *L. casei* DHFR—MTX—NADPH: (a) the complex of DHFR with the substrate H<sub>2</sub>Fol; (b) the complex of DHFR with the inhibitor MTX.

were revealed in the binary complexes of **1** with human DHFR,<sup>25</sup> with *E. coli* DHFR,<sup>11</sup> and with the enzyme species isolated from other sources. Long-lived water molecules were also detected by NMR spectroscopy in solutions of complexes of *L. casei* DHFR<sup>60</sup> and human DHFR.<sup>61</sup> The fact that the above-mentioned water molecules were also found in solutions indicates that they are strongly coordinated and confirms the assumption that they can be involved in the proton transfer to the N(5) atom.

It should be noted that the position of the water molecule found experimentally does not correspond to the position of the molecule shown in Scheme 3 as a mediator of the proton transfer to the N(5) atom through the formation of the enol form of the substrate. Based on the above conclusions, the possibility of the involvement of the keto-enol tautomerism in the mechanism of protonation at the N(5) atom of the dihydropteridine ring in **2** cannot be ruled out. The reason is that it is impossible to study the structure and the physicochemical properties of the key complex DHFR—H<sub>2</sub>Fol—NADPH as such because of the high rate of the enzymatic reaction, whereas models of the substrate and/or the coenzyme cannot assure the identity with the above-mentioned complex. The electronic state of the carboxy group of the residue Asp26 in the complex of *L. casei* DHFR with H<sub>2</sub>Fol was studied by NMR spectroscopy.<sup>62</sup> The results obtained allowed the conclusion that the pteridine fragment of the substrate, which interacts with the above-mentioned carboxy group in the binary complex, is strongly polarized. The authors believed that this polarization is the driving force for enolization of the C(4)=O carbonyl group of the substrate proceeding even in the presence of the coenzyme. A network of hydrogen bonds involving the O(4) and N(5) atoms and the water molecule, which is analogous to that shown in Scheme 3, causes the proton transfer to the N(5) atom. An analogous conclusion was also made based on analysis of the Raman spectra and *ab initio* quantum-chemical calculations.<sup>63</sup> However, the structural factors, which are responsible for the rise of pK<sub>a</sub> for protonation of **2** at the N(5) atom by four units, remain unknown. No potential acceptors of the hydrogen bond in the vicinity of the N(5) atom were revealed. The water molecule whose arrangement is favorable for coordination to the O(4) and N(5) atoms was found only in the X-ray structure of the binary complex of *E. coli* DHFR with 5-deazafolate (DZF, see Table 1).<sup>9</sup> However, the detection of this molecule posed new questions rather than provided the answer to the questions raised. For example, why this molecule was observed only in the complex in which the N(5) atom is replaced by the carbon atom (and, consequently, an efficient hydrogen bond cannot occur) is not understood. Hence, in spite of the abundant data, the aspects of the mechanism of substrate protonation, which is the stage determining the rate of the subsequent hydride-ion transfer, are not entirely known.

**3.4. The mechanism of the hydride-ion transfer from the coenzyme to the substrate.** The hydride-ion transfer from the coenzyme to the substrate was thoroughly investigated by quantum-chemical methods. The structure of the transition state and the energy profile of this reaction were studied by the semiempirical AM1 and PM3 methods,<sup>64</sup> the Hartree–Fock method,<sup>65</sup> and the combined quantum mechanics/molecular mechanics (QM/MM) methods.<sup>65–67</sup> The barrier of the transition state was estimated<sup>65,67</sup> at 110–130 kJ mol<sup>−1</sup>. In all theoretical studies in which calculations were carried out taking into account the structure of the enzyme active site,<sup>68–70</sup> substantial polarization of the substrate in the course of the reaction and the role of the carboxy group of the aspartic (glutamic) acid residue in stabilization of the charged initial and transition states were emphasized. It was assumed<sup>67</sup> that, although several amino acid residues can make contributions to the free energy through Coulomb interactions, only the interaction between the conserved carboxy group and the protonated substrate can contribute significantly to this energy (up to 40 kJ mol<sup>−1</sup>).

**3.5. Interactions between the coenzyme and the protein.** The structural and kinetic changes, which are caused by the replacements of the conserved amino acid residues (Tyr100, Ser49, and Ile14 in *E. coli* DHFR) surrounding NADPH,<sup>71</sup> in the active site revealed the Coulomb and hydrophobic interactions between the coenzyme and the protein. It was assumed that the residue Tyr100 (tyrosine or phenylalanine in all forms of the enzyme) interacts with the nicotinamide ring of the coenzyme and with the dihydropteridine ring of the substrate through the π-aromatic systems. The replacement of the aromatic amino acid by glycine or isoleucine leads to disruption of the above-mentioned interactions and to a decrease in the catalytic activity. It was also found that the tyrosine residue contributes significantly to the specificity of binding of the reduced and oxidized forms of the coenzyme. The replacements of this residue by nonaromatic residues result in the loss of the difference in the specificity of binding of NADPH and NADP<sup>+</sup> to the enzyme, which is of importance for the mechanism of catalysis. The residue Ser49 forms hydrogen bonds with the nicotinamide fragment involving a water molecule,<sup>72</sup> which can enhance stabilization of the transition state. However, the replacement of this residue by alanine did not lead to an increase in the activation barrier of the transition state in the hydride-ion transfer but promoted exit of the molecule of oxidized coenzyme NADP<sup>+</sup> resulting finally in the enhancement of the catalytic activity of the enzyme. It was assumed that Ile14, which is the strictly conserved amino acid residue in all DHFR forms, is also involved in stabilization of the transition state through hydrogen bonding with the nicotinamide fragment. It was established that the replacement of isoleucine by alanine influences the binding of NADPH to the enzyme and, in addition, decreases the rate of the hydride-ion transfer.

However, the reliable data on the reasons for the difference in the strength of binding of the reduced ( $\text{NADPH}$ ) and oxidized ( $\text{NADP}^+$ ) forms of the coenzyme to the protein are lacking. It is known that binding of **8** to all DHFR forms is several thousand times stronger compared to binding of its oxidized form **9**. Thus, the constants of binding of **8** and **9** to the enzyme from *L. casei* differ by a factor of ~5000.<sup>41</sup> At the same time, the complexes of DHFR with the oxidized and reduced forms of the coenzyme have virtually identical structures, which does not allow one to reveal the structural factors responsible for such a large difference in the strength of binding. This problem remains to be solved.

**3.6. Molecular motions and DHFR catalysis.** In the catalytic cycle, the conformation of the enzyme changes to a greater or lesser extent on going from one state to another and, hence, molecular motions necessarily play an important role in the mechanism of catalysis. This conclusion was experimentally confirmed based on a number of enzyme systems. The molecular motions in DHFR complexes and their role in the mechanism of catalysis have also been studied extensively.

Thus investigations of the conformational lability of the apo form of *E. coli* DHFR by NMR spectroscopy demonstrated that the loop I (which is located between the  $\beta$ -sheet **a** and the  $\alpha$ -helix B; see Fig. 3) oscillates with a frequency comparable with  $k_{\text{cat}}$ .<sup>73</sup> This loop plays a crucial role in the mechanism of catalysis because it forms a fragment of the enzyme active site. This loop contains the amino acid residues interacting both with the substrate and the coenzyme. Thus the strictly conserved Ile and Gly residues (13 and 14 in the enzyme from *L. casei*) are located at the beginning of the loop I; these residues are bound to the nicotinamide fragment of NADPH. This loop terminates in three conserved residues (Leu19, Pro20, and Trp21), which form the substrate binding site. It should be emphasized that the tryptophan residue is of primary importance in the mechanism of substrate protonation by coordinating a water molecule (see Fig. 7). It was suggested<sup>73</sup> that the molecular motions of the loop I can be the limiting factor in the catalytic reaction, which determines the rate of dissociation of the reaction product and, consequently, the overall reaction rate. The opening of the loop I can be initiated due to binding of NADPH to the DHFR–H<sub>4</sub>Fol complex.

The structure of *E. coli* DHFR was studied<sup>6</sup> by X-ray diffraction analysis with the aim of revealing the changes, which occur on going from the apo-enzyme to its binary complexes with  $\text{NADP}^+$  and MTX and to the ternary complex DHFR–Fol–NADP<sup>+</sup>. It was established that the structural changes of the protein upon binding of the ligands to the apo-enzyme are, on the whole, insignificant (on the average, are at most 1 Å). However, if the protein molecule is arbitrarily divided into the adenosine-binding and substrate-binding domains, the transformation from the apo-enzyme to its complexes

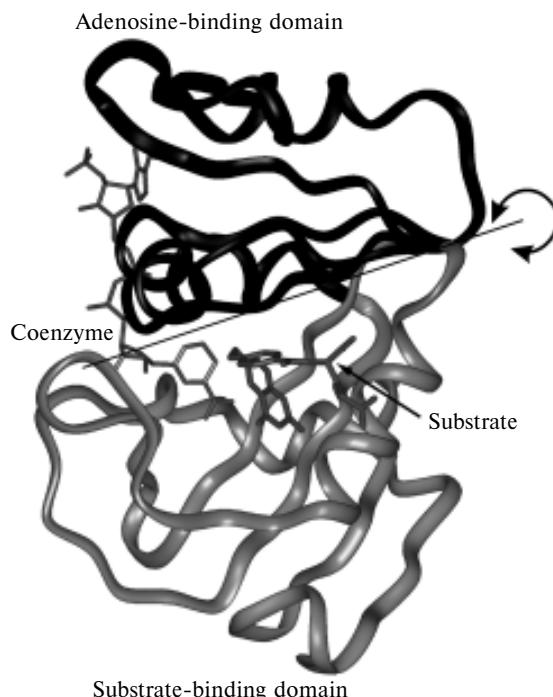


**Fig. 8.** The structure of the protein chain (the ribbon representation) of *E. coli* DHFR in the ternary complex with  $\text{NADP}^+$  and folate. The adenosine-binding domain is shaded; the substrate-binding and catalytic domains are light colored. The axis of rotation of two domains with respect to one another on going from the apo-enzyme to the ternary complex is shown.<sup>6</sup>

can be characterized by the change in the mutual orientation of these domains with the rotation axis shown in Fig. 8. The most substantial rotation (up to 7°) was observed in the complexes with MTX. In the complexes with  $\text{NADP}^+$  and H<sub>2</sub>Fol–NADP<sup>+</sup>, the angle of the mutual rotation of the domains is 4.5°.<sup>6</sup> Binding both of the coenzyme and the inhibitor leads to a decrease in the volume of the active site. In this case, the loop located between the  $\alpha$ -helix C and the  $\beta$ -sheet **c** approaches the  $\alpha$ -helix B. In the case of binding of MTX to the enzyme, this fact can be readily explained by strong Coulomb and hydrophobic interaction both with this loop and the  $\alpha$ -helix B (see Section 4.1). In the case of binding of the coenzyme, the observed structural changes occur, apparently, due to long-range effects.

In the cited study,<sup>6</sup> an attempt was made to follow the structural changes of the protein in the course of the catalytic cycle. For this purpose, crystals of complexes with *E. coli* DHFR were prepared. These complexes modeled five major kinetic intermediates. Among them are the holoenzyme DHFR–NADPH, the Michaelis complex DHFR–H<sub>2</sub>Fol–NADPH, the ternary complex of the reaction products DHFR–H<sub>4</sub>Fol–NADP<sup>+</sup>, the binary complex DHFR–H<sub>4</sub>Fol, and the ternary complex DHFR–H<sub>4</sub>Fol–NADPH. The kinetic intermediates under study included also the transition state of the hydride-ion transfer. The structures of 24 complexes

of *E. coli* DHFR were established by X-ray diffraction analysis. The authors believed that these complexes can serve as models of the above-mentioned states in six different crystalline forms.<sup>11</sup> The selected results of this investigation are schematically represented in Fig. 9. It was established that the largest structural changes of the protein in the course of the catalytic cycle are observed for the loop I and the mutual orientation of the domains, which agrees with the above-considered results. The geometry of the loop I changes and the loop is transformed from the closed to the occluded state, which corresponds to the conversion of the  $\beta$ -sheet conformation of the central portion of the loop to the  $3_{10}$ -helix. It was assumed that the structural changes of the loop involve also the formation of the most widespread open conformation (Fig. 10) of an irregular character. On going from one conformation to another, the loop can bind a water molecule, which participates in subsequent protonation of **2**. The motions of the catalytic loop are accompanied by the reorientation of the domains of the

enzyme. Thus, the volume of the active site decreases upon binding of the substrate or the reaction product, whereas the  $\alpha$ -helices B and C slightly move apart (by  $\sim 0.5$  Å) in the absence of the substrate and the reaction product, thus increasing the volume of the catalytic cavity. The authors<sup>11</sup> created the animation, which clearly demonstrates the conformational changes of the protein, which occur in the course of the catalytic reaction (see <http://chem-faculty.ucsd.edu/kraut/dhfr.html>). If it were not for a number of assumptions made, the cited study would provide exhaustive answers to most of the questions associated with the protein dynamics and its role in the mechanism of catalysis. This primarily refers to the choice of the complexes, which model the key kinetic intermediates and the reaction transition state. By the physicochemical properties, most of these complexes cannot serve as adequate models of the corresponding intermediates. For example, the transition state was modeled by the ternary complex DHFR—MTX—NADPH in which the pteridine residue is rotated by almost  $180^\circ$

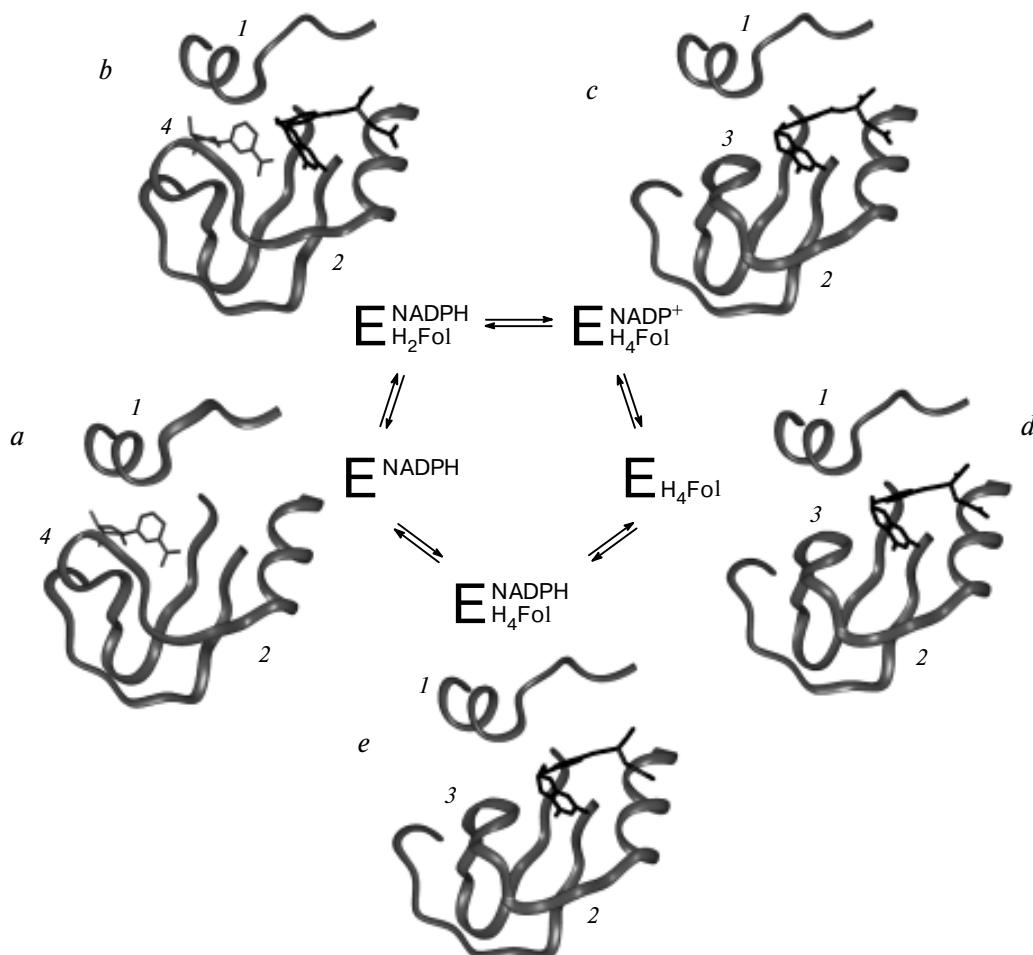


**Fig. 9.** Structural changes of the active site in *E. coli* DHFR in the course of the catalytic cycle. The arrangement of the fragment of the protein backbone and the ligands in the X-ray structures of the models of kinetic intermediates: (a) the complex with NADPH; (b) the complex with folate and NADP<sup>+</sup>; (c) the complex with 5,10-dideazatetrahydrofolate (DDF) and ATP ribose; (d) the complex with DDF; (e) the complex with DDF and NADPH. The structures are superimposed by the protein backbones of the central  $\beta$ -sheets. 1, the  $\alpha$ -helix C; 2, the  $\alpha$ -helix B; 3, the loop I (occluded); 4, the loop I (closed).

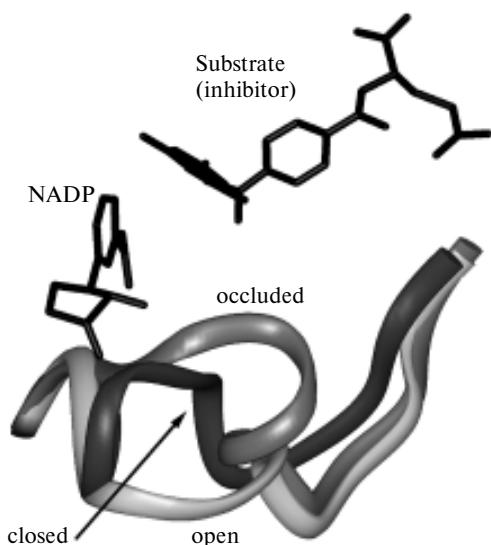


**Fig. 10.** Three main types of the protein chain (the ribbon representations) of the catalytic loop: open, closed, and occluded. The drawings were based on the atomic coordinates of the X-ray structures of the complexes of *E. coli* DHFR with NADPH (open), with NADPH and MTX (closed), and with DDF (occluded)<sup>11</sup> (Brookhaven PDB codes 1rh3, 1ra1, and 1rx5, respectively).

compared to the complex of the enzyme with the substrate. In addition, the hybridization of the N(5) and C(6) atoms and, consequently, the orientation of the bonds involving these atoms are radically different in MTX and the reaction transition state. The incorrectness of this model is also evidenced by the fact that the complex with the coenzyme and MTX is one of the most energetically favorable states of the enzyme, whereas the transition state corresponds to the maximum on the energy profile of the reaction. Analogous comments are true for most of other models used. An additional prob-

lem is the effect of the crystal packing on the geometry of the protein chains. Thus the authors obtained radically different conformations of the loop I for the same complexes in different crystalline forms. It is apparent that the data on the structures and the dynamics of the DHFR complexes in solutions are required. Hence, despite the obvious significance of the information obtained, the role of molecular motions in the mechanism of DHFR catalysis calls for further investigation.

#### 4. Interactions of DHFR with inhibitors

The first DHFR inhibitor, *viz.*, aminopterin, was synthesized in the late 1940s based on the structural analogy with substrate **1**.<sup>74</sup> This compound and MTX (**4**, the *N*-methyl analog of aminopterin), which has been synthesized a short time later,<sup>75</sup> showed high efficiency in the treatment of leukemia and some other tumor diseases. Since then, MTX is still among the most important antitumor drugs used in medicine.<sup>33</sup> In 1950s, other antifolate pharmaceuticals were also designed, including the important antibacterial drug TMP. Studies of the mechanism of functioning of these drugs demonstrated that they serve as competitive DHFR inhibitors. The discovery of antagonists of folic acid gave impetus to further investigations of the mechanism of catalysis.

**4.1. Characteristics of interactions of MTX with DHFR.** As mentioned above, binding of MTX to the enzyme is exclusively strong. For its binary complex (**4**—DHFR from *L. casei*),  $K_d \approx 5 \cdot 10^{-10}$  mol L<sup>-1</sup>,<sup>76</sup> whereas the constants  $K_d$  for ternary complexes with NADPH and the eukaryotic enzymes fall to  $10^{-11}$  mol L<sup>-1</sup><sup>35</sup> and, hence, cannot be accurately measured. Such a strong binding results from a number of specific interactions between the inhibitor and the amino acid residues of the protein (Fig. 11). In the complex with the enzyme, methotrexate (**4**) is

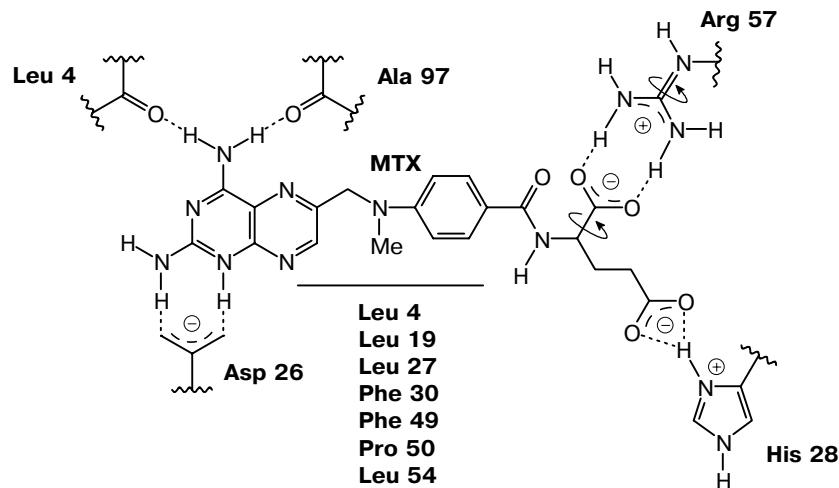
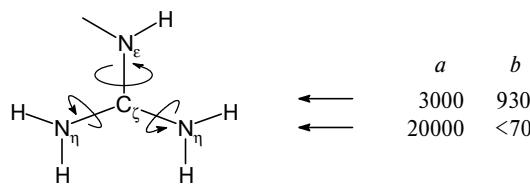


**Fig. 11.** Interactions of MTX with amino acid residues of *L. casei* DHFR. Only direct contacts between the inhibitor and the protein (water molecules are omitted) are shown, including the amino acid residues involved in hydrophobic interactions with the pteridine and phenyl residues of MTX. The synchronized rotations of the bonds are indicated by arrows.

porotonated at the N(1) atom, which is responsible for the efficient Coulomb interaction with the carboxy group of the aspartic (glutamic) acid residue. On going from the free to the bound state,  $pK_a$  of MTX is increased by more than 5 units (from 5.3 to 10.5 in the complex with the *L. casei* enzyme).<sup>77</sup> In the NMR spectra of the complex of *L. casei* DHFR with MTX, the signal for the H atom at N(1) has the chemical shift of approximately 17 ppm, which indicates that this atom is involved in strong hydrogen bonding.<sup>15</sup> The geometry and the energy of this interaction were studied<sup>78</sup> by the PM3 semiempirical quantum-mechanical method.

The Coulomb interactions of the  $\alpha$ - and  $\gamma$ -carboxy groups of the *p*-methylaminobenzoylglutamine residue of the inhibitor with the positively charged residues His28 and Arg57 (see Fig. 11) also play an important role in the binding of MTX to the enzyme. The replacement of the  $\gamma$ - and  $\alpha$ -carboxy groups by amide groups leads to a decrease in the constant of binding of the resulting analogs of MTX by one and two orders of magnitude, respectively.<sup>79</sup> This corresponds to the interaction energies of  $\sim 5.7$  and  $\sim 11.4$  kJ mol<sup>-1</sup> for the  $\gamma$ - and  $\alpha$ -carboxy groups, respectively. Both interactions were thoroughly studied by NMR spectroscopy.<sup>80</sup> Thus  $pK_a$  of the imidazole ring of the residue His28 in complexes with MTX is  $\sim 1$  unit higher than those in the apo-enzyme or in the complexes with ligands deprived of the  $\gamma$ -carboxy group.<sup>81</sup> It should be noted that His28 is not a strictly conserved residue and the above-mentioned interaction may be absent in some bacterial forms of the enzyme. At the same time, the interaction between the  $\alpha$ -carboxy group and the positively charged guanidine fragment of the arginine residue is observed for the enzymes from all sources. The geometry and the dynamic characteristics of this interaction were studied in detail by NMR spectroscopy.<sup>82–84</sup> In particular, it was established that the interacting groups synchronize the bond rotations (indicated by arrows in Fig. 11). On going from free arginine (*a*) to the complex (*b*) in which this residue interacts with the carboxy groups, the rate of rotation ( $s^{-1}$ ) about the  $N_e-C_\zeta$  bond changes only slightly, whereas the rotation about the  $C_\zeta-N_\eta$  bond slows down by a factor of  $\sim 300$ .



This fact can be explained exclusively by synchronous rotation of the guanidine group of the arginine residue and the carboxy group of MTX proceeding without disruption of the interaction between these fragments. This correlated rotation of the interacting fragments provides the high energy of binding due to an

increase in the entropy of the system, its enthalpy remaining unchanged.

Hydrophobic interactions of the pteridine and benzoyl rings of the inhibitor with the lipophilic amino acid residues involved in the enzyme active site contribute significantly to the total energy of binding of MTX to DHFR. The key residues ensuring efficient hydrophobic interactions with the inhibitor are Leu27, Phe30, Phe49, and Leu54 (the numbering scheme was used for *L. casei* DHFR) with the total energy of no lower than 10.5 kJ mol<sup>-1</sup>.<sup>33</sup> Most of the above-mentioned residues are conserved and even their replacements by residues, which are similar in structure or properties, lead to noticeable changes in the specificity of binding. Thus the kinetic studies of the *E. coli* enzyme in which the residue Phe31 (an analog of Phe30 in the *L. casei* enzyme) is replaced by Tyr or Val showed that these replacements lead to weakening of the hydrophobic interactions both with the inhibitor and the substrate.<sup>85</sup>

**4.2. Interactions of nonclassical antifolate pharmaceuticals with DHFR.** Being a close structural analog of endogenous metabolites of **1**, methotrexate penetrates into a cell *via* the active transport used for delivering folates and leucovorin (5-formyl-5,6,7,8-tetrahydrofolic acid). This transport system is based on the formation of polyglutamine derivatives catalyzed by the enzyme folyl-polyglutamate synthetase.<sup>86</sup> A decrease in activity of this enzyme is the main reason for the appearance of cell stability with respect to MTX.<sup>87</sup> New lipophilic antifolate pharmaceuticals are free from these drawbacks. These drugs are devoid of the glutamine residue due to which they do not employ the folate active transport for penetrating through the cell membrane. Recently, several new drugs of this class have been designed among which TMQ (**5**) is noteworthy. This compound was successfully put through clinical trials and was permitted to use in medical practice. Trimethrexate was first synthesized as a potential antimalarial drug.<sup>88</sup> More recently, this drug proved to be efficient in the treatment of malignant tumors of mamma, brain, and neck<sup>89</sup> and to exhibit antibacterial activity in the treatment of pneumonia in HIV-infected patients.<sup>90</sup>

The mechanism of functioning of **5** is also based on DHFR inhibition. The examination of the inhibiting properties of this drug demonstrated that, though possessing the inhibiting activity, which is approximately an order of magnitude lower than that of MTX, it is still very strongly bound to the enzyme.<sup>91</sup> The constant of dissociation of the inhibitor from the binary complex with *L. casei* DHFR was measured by the competitive binding method ( $K_d \approx 5 \cdot 10^{-9}$  mol L<sup>-1</sup>).<sup>16</sup>

The high-resolution structure of the complex TMQ—DHFR from *L. casei* in solution was established by NMR spectroscopy.<sup>16,92</sup> The orientation of the quinazoline fragment of the inhibitor within the binding site of the protein is similar to that of the pteridine residue of MTX (Fig. 12). The internuclear contacts between the protons of inhibitor **5** and the protein,

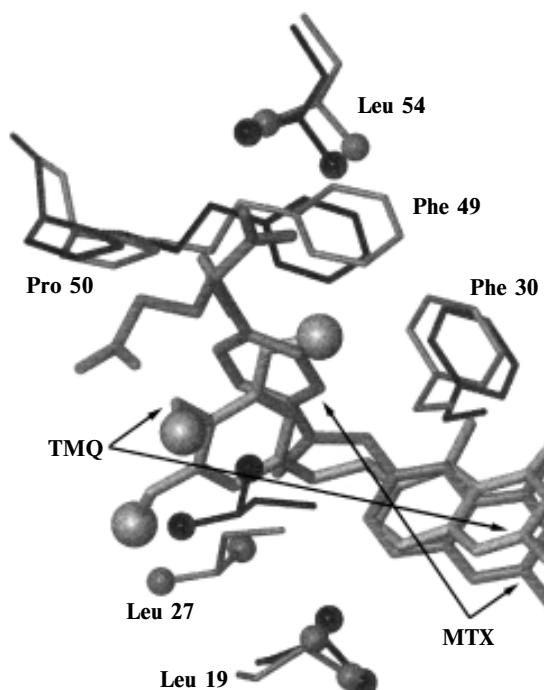


**Fig. 12.** The compounds TMQ and MTX located in the binding site of *L. casei* DHFR. The side chains of the residues involved in hydrophobic contacts with TMQ and MTX are shown. The methyl groups are presented by spheres. The complex DHFR—MTX is dark colored. The structures of the complexes DHFR—TMQ and DHFR—MTX are superimposed by the protein backbones.\*

which were established based on analysis of the nuclear Overhauser effects, are shown in Fig. 13. It can be seen that the TMQ molecule is surrounded primarily by lipophilic residues, which is indicative of a substantial contribution of hydrophobic interactions to the total energy of substrate binding. The loss of two sites of Coulomb interactions involving the carboxy groups on going from **4** to **5** is equivalent to the lowering of the binding energy by  $\sim 17 \text{ kJ mol}^{-1}$  (see Section 4.2). At the same time, the binding constant of **4** is only an order of magnitude smaller than that of **5**, which corresponds to the change of the binding energy by  $\sim 5.7 \text{ kJ mol}^{-1}$ . Therefore, the hydrophobic interaction of **5** with the protein is more efficient than that of **4** (the difference between the energies is larger than  $11 \text{ kJ mol}^{-1}$ ). Similar quantitative estimates of the difference between the energies of the hydrophobic interactions of **4** and **5** with *L. casei* DHFR were obtained based on analysis of the molecular motions of the inhibitors within the active site of the protein. Thus the rate of the turn-over of the aromatic rings of the inhibitors depends on the strength of their specific interactions (primarily, of hydrophobic interactions) with the protein. These interactions must be broken upon the turn-over of the ring, and analysis of the temperature dependences of the rates of molecu-

\* Courtesy of Polshakov *et al.*<sup>16</sup>

lar motions made it possible to estimate the energy of additional hydrophobic interactions of **5** at  $10\text{--}15 \text{ kJ mol}^{-1}$ .<sup>16</sup>

It should be emphasized that the secondary structure of the protein changes only slightly on going from the complex DHFR—MTX to the complex DHFR—TMQ (see Fig. 12) in spite of a significant change in the character of specific interactions between the inhibitors and the protein. Even the orientations of the side chains of the amino acid residues (the torsion angles  $\chi^1$  and  $\chi^2$ ) and their spatial arrangement vary only slightly on going from one complex to another. This indicates that the enzyme retains its secondary structure, the binding site being only insignificantly adapting to a particular ligand. Interestingly, the conformation of the ligand (TMQ) in the complex with the protein is identical with that observed in the free state.<sup>93</sup> The minimum energy expended for changing the conformations of the protein and the ligand upon complex formation is finally manifested in their high binding energy.

**4.3. Selective binding of trimethoprim (TMP) to bacterial DHFR.** Trimethoprim (2,4-diamino-5-(3,4,5-trimethoxybenzyl)pyrimidine (**6**)), which is an antibacterial drug with a broad spectrum of action, was discovered in the late 1950s.<sup>94</sup> This compound is used together with sulfanilamides as a combined drug for the treatment of respiratory, gastroenteric, and other bacterial infections. The mechanism of action of TMP is based on inhibition of bacterial DHFR. This compound possesses rather low toxicity and exhibits substantial efficiency due to higher selectivity of TMP binding to bacterial forms of the enzyme compared to human DHFR.<sup>3,94</sup> Table 3 gives the constants  $I_{50}$  for inhibition of the enzymes from various organisms under the action of TMP. It can be seen that the concentrations of the compound required for 50% inhibition of DHFR from high organisms are several orders of magnitude higher than those sufficient for bacterial forms. The constants  $I_{50}$  overestimate the differences in the specificity of TMP binding to the enzymes from eukaryotes and prokaryotes. However, it was demonstrated<sup>95</sup> that the constants of TMP binding to the above-mentioned forms also differ by a factor of 3000–12000. The high selectiv-

**Table 3.** Inhibition of various forms of DHFR with trimethoprim<sup>3</sup>

Source of DHFR	$I_{50}$ (nmol L <sup>-1</sup> )*
<i>Escherichia coli</i>	7
<i>Proteus vulgaris</i>	7
<i>Staphylococcus aureus</i>	5
Chicken	470000
Mouse	280000
Human	490000

\* The concentration of trimethoprim at which 50% inhibition of the enzyme was achieved.

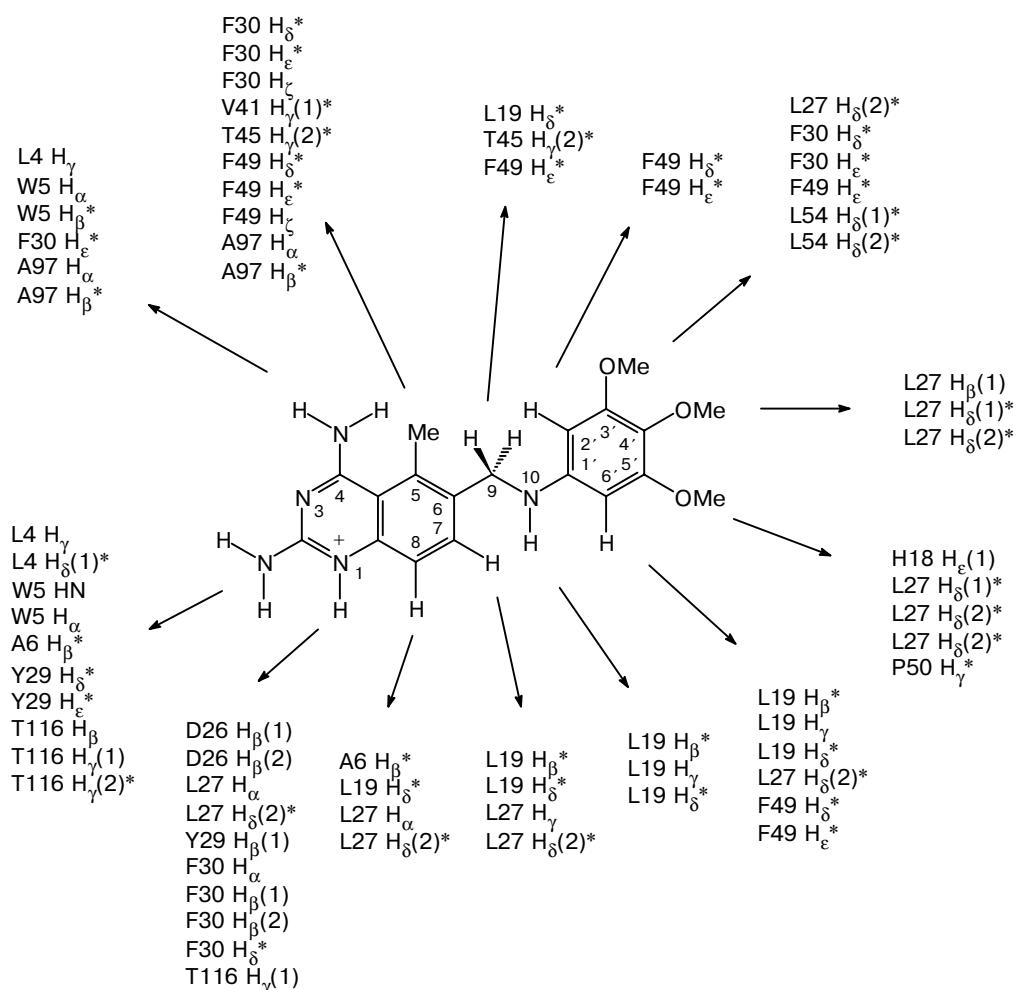


Fig. 13. Intermolecular nuclear Overhauser effects between the protons of TMQ and the protein in the complex *L. casei* DHFR—TMQ.\*

ity of TMP binding to the bacterial enzyme is to a large extent determined by the positive cooperative effect due to the interactions of TMP and NADPH with bacterial DHFR. These effects are either absent or insignificant upon binding of these ligands to eukaryotic DHFR. Due to high intracellular concentration of NADPH, the ternary complex DHFR—TMP—NADPH is formed as the major product of the interaction of the enzyme with the inhibitor, and hence, the cooperative effects of binding of these ligands play a decisive role in the mechanism of selective DHFR inhibition.

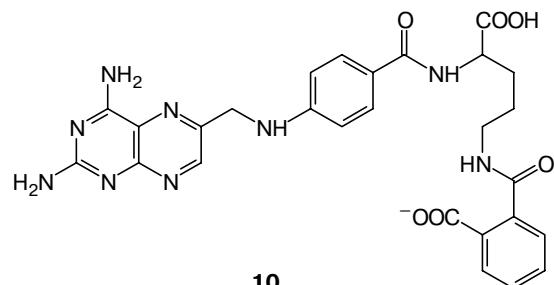
The cooperative effects either result from the direct ligand-ligand interactions or occur due to changes in the conformation of the binding site of the second ligand, which are caused by the binding of the first ligand. The mechanism of cooperative binding of TMP and NADPH was studied intensively. In particular, it was demonstrated that the binding of TMP to the complex NADPH—DHFR from *E. coli* afforded a ter-

nary complex, which is slowly isomerized to adopt a new conformation.<sup>96</sup> The NMR study showed that the complex *L. casei* DHFR—TMP—NADP<sup>+</sup> existed as two conformers, which underwent slow interconversion.<sup>97</sup> Therefore, the change in the conformation of the protein upon binding of the inhibitor and the coenzyme may play a part in the mechanism of cooperative binding of the ligands. Actually, X-ray diffraction studies showed that the conformation of the loop I in the complex of *E. coli* DHFR with TMP changes in the presence of the coenzyme NADPH so that the residue Met20 in the ternary complex forms more tight hydrophobic contacts with the methyl groups of the trimethoxyphenyl residue of the inhibitor.<sup>98</sup> Comparison of the X-ray structures of the complexes of TMP with the bacterial and avian enzymes allowed the authors to propose an interesting hypothesis for the nature of the cooperative effect of the TMP and NADPH binding.<sup>30</sup> It was demonstrated that the conformation of the inhibitor in the complex with the bacterial enzyme differs from that in the complex with the avian enzyme. In the

\* Courtesy of Polshakov *et al.*<sup>16</sup>

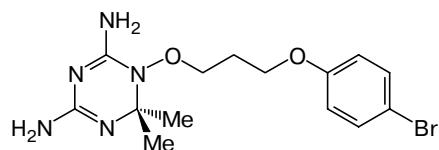
complex with the *E. coli* enzyme, the trimethoxyphenyl residue of TMP is involved in the direct contact with the coenzyme, whereas this residue in the complex with chicken DHFR is rotated toward an alternative pocket by almost 90°. It was assumed that this fact can serve as the structural basis for the selective binding of **6** to bacterial DHFR. However, the above-mentioned differences were not observed in the analogous complex with mouse DHFR.<sup>99</sup> In this case, the conformation of TMP and its specific interactions with the coenzyme and the protein appeared to be identical with those observed in the complex with the bacterial enzyme. These data cast doubt on the hypotheses proposed previously for the nature of the cooperative effect. Hence, no justified explanation for the selectivity of TMP binding is presently available. The NMR study of the character of molecular motions of TMP within the binding site of *L. casei* DHFR in the binary and ternary complexes with the coenzyme suggested that direct hydrophobic interactions with NADPH are, probably, of considerable importance in the manifestation of high specificity of TMP binding.<sup>100</sup> The data obtained were indicative also of the existence of correlated motions of the trimethoxyphenyl residue of TMP and the nicotinamide residue of NADPH in their ternary complex. Such correlated motions are absent in the complex with NADP<sup>+</sup> in which no cooperative effect of binding is observed. These data agree also with the results of microcalorimetric investigations of interactions of TMP with the bacterial and human enzymes.<sup>101,102</sup> It was shown that the selectivity of TMP binding to the bacterial enzyme is determined primarily by the entropy factors. Hence, the cooperative effects have a complex nature and are determined both by the static and dynamic factors. A deeper understanding of the nature of these effects invites further investigation.

**4.4. Structural studies and the search for new DHFR inhibitors.** Many research groups focus their efforts on the search for new more efficient DHFR inhibitors. The abundant data on the mechanism of functioning and the structure of the enzyme provided a good basis for these investigations. The structural studies in this field take two paths, *viz.*, investigations devoted to the establishment of the structures of complexes of new potential inhibitors with the enzymes whose three-dimensional structures are already known and studies aimed at determining the structures of new DHFR forms.



The structures of complexes of human DHFR with a new analog of MTX, *viz.*, PT523 (**10**), were established by X-ray diffraction analysis<sup>28</sup> and NMR spectroscopy.<sup>103</sup> This compound is of interest because its binding to the human enzyme is stronger than that of MTX. The available structural information made it possible to reveal specific interactions between the hemiphthaloyl residue of the inhibitor and the protein, which are responsible for the high ligand affinity. It was also established that the pteridine fragment is bound to the enzyme analogously to MTX, whereas the hemiphthaloyl residue can exist as three conformers.

An interesting study was devoted to the structures of the complexes of MTX, TMP, and the potential antimalarial drug WRB (**11**) with DHFR from microbacteria *Mycobacterium tuberculosis*.

**11**

The X-ray structures of the above-mentioned complexes were compared with the analogous structures of human DHFR. In spite of the fact that the amino acid sequences of these two enzymes are only 26% homologous, their structures are similar. However, a number of essential differences were revealed. Among them are the more hydrophobic character of the binding site of the nicotinamide coenzyme and a larger volume of the inhibitor binding site in the *M. tuberculosis* enzyme compared with the human enzyme. Thus, this additional pocket in the binary complex DHFR-MTX is occupied by the glycerol molecule, which was used as a component of the solvent in the crystallization of the protein. The above-mentioned differences can be used in the rational search for new DHFR inhibitors possessing antitubercular activity.

In recent years, NMR spectroscopy has played an important role in structural studies. This method allows one to carry out complete calculations for the structures of the DHFR complexes in solution<sup>15,16</sup> and to determine the position of the inhibitor within the protein binding site.<sup>14,92,103,104</sup> Recently, a new efficient procedure for the design of strongly bound inhibitors with the use of NMR spectroscopy has been developed.<sup>105,106</sup> According to this procedure, a series of ligands is examined from the viewpoint of their binding to the target of action using changes in the <sup>15</sup>N and <sup>1</sup>H chemical shifts of the protein to establish the position of the ligand binding site. Once the best ligand is chosen, the enzyme is saturated with this compound and an analogous search for the second ligand, which is noncompetitively bound to an alternative site of the protein, is performed. Once the second ligand is chosen and the position of its binding site is revealed, a linker is selected such that it

can bind both fragments without disturbing their positions in the protein molecule. Out of several compounds involving two initial fragments and the linker, the optimum compound is chosen. The latter, as a rule, is very strongly bound to the enzyme. This method proved to be efficient in the search for inhibitors of a number of enzymes<sup>107–109</sup> and it, undeniably, can be used to good advantage in the search for new DHFR inhibitors.

### 5. Unresolved problems and the lines of further investigations

The data surveyed in the present review demonstrate that, in spite of the abundant information on the subject, many important problems still remain to be solved. For example, the structural factors responsible for a substantial increase in  $pK_a$  of the substrate in the complex with the enzyme are unknown, the reasons for the existence of the cooperative effects of ligand binding remain to be revealed, reliable data on the molecular motions of the protein and their role in the catalysis mechanism are lacking, etc. The above problems will be, undoubtedly, solved and will allow one to gain a better understanding of the fundamental biochemical processes. However, it should be emphasized that the rational search for inhibitors of enzymes requires a detailed knowledge of the objects under study. Recently, the belief has been stated that information on the amino acid sequence of the potential binding target can be applied to the development of a protein model using homology methods and that such a model can be used as the basis for the determination of the structure of the compound, which could be efficiently bound to the target. The above-surveyed data indicate that this point of view is unjustified and unreasonable. Rational procedures for the search for new drugs should be based on precise structural data and a fundamental knowledge of the molecular recognition processes.

The author acknowledges valuable advice and comments from James Feeney and Berry Birdsall.

This study was financially supported by the Horward Hughse Medical Institute (USA, Grant 75195-546701) and by the Russian Foundation for Basic Research (Project No. 99-04-48288).

### References

- R. L. Blakley, *Chemistry and Biochemistry of Folates*, in *Folates and Pterins*, Wiley, New York, 1984, 191.
- G. H. Hitchings, *Angew. Chem., Int. Ed. Engl.*, 1989, **28**, 879.
- D. P. Baccanari and L. F. Kuyper, *J. Chemother.*, 1993, **5**, 393.
- J. T. Bolin, D. J. Filman, D. A. Matthews, R. C. Hamlin, and J. Kraut, *J. Biol. Chem.*, 1982, **257**, 13650.
- C. Bystroff, S. J. Oatley, and J. Kraut, *Biochemistry*, 1990, **29**, 3263.
- C. Bystroff and J. Kraut, *Biochemistry*, 1991, **30**, 2227.
- M. S. Warren, K. A. Brown, M. F. Farnum, E. E. Howell, and J. Kraut, *Biochemistry*, 1991, **30**, 11092.
- K. A. Brown, E. E. Howell, and J. Kraut, *Proc. Natl. Acad. Sci. USA*, 1993, **90**, 11753.
- V. M. Reyes, M. R. Sawaya, K. A. Brown, and J. Kraut, *Biochemistry*, 1995, **34**, 2710.
- H. Lee, V. M. Reyes, and J. Kraut, *Biochemistry*, 1996, **35**, 7012.
- M. R. Sawaya and J. Kraut, *Biochemistry*, 1997, **36**, 586.
- J. Dunbar, H. P. Yennawar, S. Banerjee, J. Luo, and G. K. Farber, *Protein Sci.*, 1997, **6**, 1727.
- D. A. Matthews, R. A. Alden, J. T. Bolin, D. J. Filman, S. T. Freer, R. Hamlin, W. G. Hol, R. L. Kisliuk, E. J. Pastore, L. T. Plante, N. Xuong, and J. Kraut, *J. Biol. Chem.*, 1978, **253**, 6946.
- W. D. Morgan, B. Birdsall, V. I. Polshakov, D. Sali, I. Kompis, and J. Feeney, *Biochemistry*, 1995, **34**, 11690.
- A. R. Gargaro, A. Soteriou, T. A. Frenkel, C. J. Bauer, B. Birdsall, V. I. Polshakov, I. L. Barsukov, G. C. Roberts, and J. Feeney, *J. Mol. Biol.*, 1998, **277**, 119.
- V. I. Polshakov, B. Birdsall, T. A. Frenkel, A. R. Gargaro, and J. Feeney, *Protein Sci.*, 1999, **8**, 467.
- J. N. Champness, A. Achari, S. P. Ballantine, P. K. Bryant, C. J. Delves, and D. K. Stammers, *Structure*, 1994, **2**, 915.
- V. Cody, N. Galitsky, J. R. Luft, W. Pangborn, A. Gangjee, R. Devraj, S. F. Queener, and R. L. Blakley, *Acta Crystallogr., Sect. D*, 1997, **53**, 638.
- V. Cody, N. Galitsky, D. Rak, J. R. Luft, W. Pangborn, and S. F. Queener, *Biochemistry*, 1999, **38**, 4303.
- V. Cody, D. Chan, N. Galitsky, D. Rak, J. R. Luft, W. Pangborn, S. F. Queener, C. A. Laughton, and M. F. Stevens, *Biochemistry*, 2000, **39**, 3556.
- R. Li, R. Sirawaraporn, P. Chitnumsub, W. Sirawaraporn, J. Wooden, F. Athappilly, S. Turley, and W. G. Hol, *J. Mol. Biol.*, 2000, **295**, 307.
- T. Dams, G. Auerbach, G. Bader, U. Jacob, T. Ploom, R. Huber, and R. Jaenicke, *J. Mol. Biol.*, 2000, **297**, 659.
- M. Whitlow, A. J. Howard, D. Stewart, K. D. Hardman, L. F. Kuyper, D. P. Baccanari, M. E. Fling, and R. L. Tansik, *J. Biol. Chem.*, 1997, **272**, 30289.
- U. Pieper, G. Kapadia, M. Mevarech, and O. Herzberg, *Structure*, 1998, **6**, 75.
- C. Oefner, A. D'Arcy, and F. K. Winkler, *Eur. J. Biochem.*, 1988, **174**, 377.
- J. F. D. Davies, T. J. Delcamp, N. J. Prendergast, V. A. Ashford, J. H. Freisheim, and J. Kraut, *Biochemistry*, 1990, **29**, 9467.
- W. S. Lewis, V. Cody, N. Galitsky, J. R. Luft, W. Pangborn, S. K. Chunduru, H. T. Spencer, J. R. Appleman, and R. L. Blakley, *J. Biol. Chem.*, 1995, **270**, 5057.
- V. Cody, N. Galitsky, J. R. Luft, W. Pangborn, A. Rosowsky, and R. L. Blakley, *Biochemistry*, 1997, **36**, 13897.
- A. Gangjee, A. P. Vidwans, A. Vasudevan, S. F. Queener, R. L. Kisliuk, V. Cody, R. Li, N. Galitsky, J. R. Luft, and W. Pangborn, *J. Med. Chem.*, 1998, **41**, 3426.
- D. A. Matthews, J. T. Bolin, J. M. Burridge, D. J. Filman, K. W. Volz, B. T. Kaufman, C. R. Beddell, J. N. Champness, D. K. Stammers, and J. Kraut, *J. Biol. Chem.*, 1985, **260**, 381.
- M. A. McGigue, J. F. D. Davies, B. T. Kaufman, and J. Kraut, *Biochemistry*, 1992, **31**, 7264.
- M. A. McGigue, J. F. D. Davies, B. T. Kaufman, and J. Kraut, *Biochemistry*, 1993, **32**, 6855.

33. F. M. Huennekens, *Adv. Enzyme Regul.*, 1994, **34**, 397.
34. G. C. K. Roberts, J. Feeney, B. Birdsall, P. Charlton, and D. W. Yaung, *Nature*, 1980, **286**, 309.
35. B. I. Schweitzer, A. P. Dicker, and J. R. Bertino, *FASEB J.*, 1990, **4**, 2441.
36. J. G. Dann, G. Ostler, R. A. Bjur, R. W. King, P. Scudder, P. C. Turner, G. C. K. Roberts, A. S. V. Burgen, and N. G. L. Harding, *Biochem. J.*, 1976, **157**, 559.
37. S. D. Varfolomeev and K. G. Gurevich, *Biokinetika. Prakticheskii kurs [Biokinetics. Practical Course]*, Far-press, Moscow, 1999, 716 pp. (in Russian).
38. C. A. Fierke, K. A. Johnson, and S. J. Benkovic, *Biochemistry*, 1987, **26**, 4085.
39. S. J. Benkovic, C. A. Fierke, and A. M. Naylor, *Science*, 1988, **239**, 1105.
40. C. R. Wagner, J. Thillet, and S. J. Benkovic, *Biochemistry*, 1992, **31**, 7834.
41. J. Andrews, C. A. Fierke, B. Birdsall, G. Ostler, J. Feeney, G. C. K. Roberts, and S. J. Benkovic, *Biochemistry*, 1989, **28**, 5743.
42. S. A. Margosiak, J. R. Appleman, D. V. Santi, and R. L. Blakley, *Arch. Biochem. Biophys.*, 1993, **305**, 499.
43. J. Thillet, J. A. Adams, and S. J. Benkovic, *Biochemistry*, 1990, **29**, 5195.
44. J. R. Appleman, W. A. Beard, T. J. Delcamp, N. J. Prendergast, J. H. Freisheim, and R. L. Blakley, *J. Biol. Chem.*, 1990, **265**, 2740.
45. B. Birdsall, A. S. Burgen, E. I. Hyde, G. C. Roberts, and J. Feeney, *Biochemistry*, 1981, **20**, 7186.
46. E. J. Pastore and M. Friedkin, *J. Biol. Chem.*, 1962, **237**, 3002.
47. P. A. Charlton, D. W. Young, B. Birdsall, J. Feeney, and G. C. K. Roberts, *J. Chem. Soc., Perkin Trans. 1*, 1985, 1349.
48. J. E. Villafranca, E. E. Howell, D. H. Voet, M. S. Strobel, R. C. Ogden, J. N. Abelson, and J. Kraut, *Science*, 1983, **222**, 782.
49. E. E. Howell, J. E. Villafranca, M. S. Warren, S. J. Oatley, and J. Kraut, *Science*, 1986, **231**, 1123.
50. G. Maharaj, B. S. Selinsky, J. R. Appleman, M. Perlman, R. E. London, and R. L. Blakley, *Biochemistry*, 1990, **29**, 4554.
51. J. E. Gready, *J. Comput. Chem.*, 1985, **6**, 377.
52. R. L. Blakley, J. R. Appleman, J. H. Freisheim, and M. J. Jablonsky, *Arch. Biochem. Biophys.*, 1993, **306**, 501.
53. B. S. Selinsky, M. E. Perlman, R. E. London, C. J. Unkefer, J. Mitchell, and R. L. Blakley, *Biochemistry*, 1990, **29**, 1290.
54. Y. Q. Chen, J. Kraut, R. L. Blakley, and R. Callender, *Biochemistry*, 1994, **33**, 7021.
55. B. Birdsall, J. Feeney, S. J. B. Tendler, S. J. Hammond, and G. C. K. Roberts, *Biochemistry*, 1989, **28**, 2297.
56. H. T. Cheung, B. Birdsall, T. A. Frenkel, D. D. Chau, and J. Feeney, *Biochemistry*, 1993, **32**, 6846.
57. T. Uchimaru, S. Tsuzuki, K. Tanabe, S. J. Benkovic, K. Furukawa, and K. Taira, *Biochem. Biophys. Res. Commun.*, 1989, **161**, 64.
58. Y. Q. Chen, J. Kraut, and R. Callender, *Biophys. J.*, 1997, **72**, 936.
59. B. Birdsall, M. G. Casarotto, H. T. Cheung, J. Basran, G. C. Roberts, and J. Feeney, *FEBS Lett.*, 1997, **402**, 157.
60. I. P. Gerohanassis, B. Birdsall, C. J. Bauer, T. A. Frenkel, and J. Feeney, *J. Mol. Biol.*, 1992, **226**, 549.
61. E. M. Meiering and G. Wagner, *J. Mol. Biol.*, 1995, **247**, 294.
62. M. G. Casarotto, J. Basran, R. Badii, K. H. Sze, and G. C. Roberts, *Biochemistry*, 1999, **38**, 8038.
63. H. Deng and R. Callender, *J. Am. Chem. Soc.*, 1998, **120**, 7730.
64. J. Andres, V. Moliner, V. S. Safont, L. R. Domingo, M. T. Picher, and J. Krechl, *Bioorg. Chem.*, 1996, **24**, 10.
65. R. Castillo, J. Andres, and V. Moliner, *J. Am. Chem. Soc.*, 1999, **121**, 12140.
66. P. L. Cummins and J. E. Gready, *J. Phys. Chem. B*, 2000, **104**, 4503.
67. P. L. Cummins and J. E. Gready, *J. Comput. Chem.*, 1998, **19**, 977.
68. J. Bajorath, J. Kraut, Z. Q. Li, D. H. Kitson, and A. T. Hagler, *Proc. Natl. Acad. Sci. USA*, 1991, **88**, 6423.
69. S. P. Greatbanks, J. E. Gready, A. C. Limaye, and A. P. Rendell, *Proteins — Struct. Funct. Genet.*, 1999, **37**, 157.
70. S. P. Greatbanks, J. E. Gready, A. C. Limaye, and A. P. Rendell, *J. Comput. Chem.*, 2000, **21**, 788.
71. J. A. Adams, C. A. Fierke, and S. J. Benkovic, *Biochemistry*, 1991, **30**, 11046.
72. D. J. Filman, J. T. Bolin, D. A. Matthews, and J. Kraut, *J. Biol. Chem.*, 1982, **257**, 13663.
73. C. J. Falzone, P. E. Wright, and S. J. Benkovic, *Biochemistry*, 1994, **33**, 439.
74. S. Farber, L. K. Diamond, R. D. Mercer, R. F. Sylvester, and J. A. Wolff, *Nat. Engl. J. Med.*, 1948, **238**, 787.
75. D. R. Seeger, D. B. Cosulich, J. M. Smith, J. R. Hultquist, and M. E. Hultquist, *J. Am. Chem. Soc.*, 1949, **71**, 1753.
76. B. Birdsall, A. S. Burgen, and G. C. Roberts, *Biochemistry*, 1980, **19**, 3723.
77. L. Cocco, C. Temple, Jr., J. A. Montgomery, R. E. London, and R. L. Blakley, *Biochem. Biophys. Res. Commun.*, 1981, **100**, 413.
78. V. I. Polshakov, B. Birdsall, M. J. Gradwell, and J. Feeney, *Theochem. — J. Mol. Struct.*, 1995, **357**, 207.
79. D. J. Antonjuk, B. Birdsall, H. T. A. Cheung, G. M. Clore, J. Feeney, A. Gronenborn, G. C. K. Roberts, and T. Q. Tran, *Br. J. Pharmacol.*, 1984, **81**, 309.
80. J. Feeney, *Angew. Chem., Int. Ed. Engl.*, 2000, **39**, 291.
81. A. Gronenborn, B. Birdsall, E. I. Hyde, G. C. Roberts, J. Feeney, and A. S. Burgen, *Biochemistry*, 1981, **20**, 1717.
82. A. R. Gargaro, T. A. Frenkel, P. M. Nieto, B. Birdsall, V. I. Polshakov, W. D. Morgan, and J. Feeney, *Eur. J. Biochem.*, 1996, **238**, 435.
83. P. M. Nieto, B. Birdsall, W. D. Morgan, T. A. Frenkel, A. R. Gargaro, and J. Feeney, *FEBS Lett.*, 1997, **405**, 16.
84. B. Birdsall, V. I. Polshakov, and J. Feeney, *Biochemistry*, 2000, **39**, 9819.
85. J. T. Chen, K. Taira, C. P. Tu, and S. J. Benkovic, *Biochemistry*, 1987, **26**, 4093.
86. J. J. McGuire, P. Hsieh, J. K. Coward, and J. R. Bertino, *J. Biol. Chem.*, 1980, **255**, 5776.
87. D. E. McCloskey, J. J. McGuire, C. A. Russell, B. G. Rowan, J. R. Bertino, G. Pizzorno, and E. Mini, *J. Biol. Chem.*, 1991, **266**, 6181.
88. E. F. Elslager, J. L. Johnson, and L. M. Werbel, *J. Med. Chem.*, 1983, **26**, 1753.
89. F. Robert, *Semin. Oncol.*, 1988, **15**, 22.
90. J. T. Lin and J. R. Bertino, *J. Clin. Oncol.*, 1987, **5**, 2032.
91. R. C. Jackson, D. W. Fry, T. J. Boritzki, J. A. Besserer, W. R. Leopold, B. J. Sloan, and E. F. Elslager, *Adv. Enzyme Regul.*, 1984, **22**, 187.
92. V. I. Polshakov, W. D. Morgan, B. Birdsall, and J. Feeney, *J. Biomol. NMR*, 1999, **14**, 115.

93. A. Hempel, N. Camerman, D. Mastropaoletti, and A. Camerman, *Acta Crystallogr., Sect. C*, 2000, **56**, 1225.
94. G. H. Hitchings, Jr., *Vitro Cell, Dev. Biol.*, 1989, **25**, 303.
95. D. P. Baccanari, S. Daluge, and R. W. King, *Biochemistry*, 1982, **21**, 5068.
96. S. R. Stone and J. F. Morrison, *Biochim. Biophys. Acta*, 1986, **869**, 275.
97. B. Birdsall, A. W. Bevan, C. Pascual, G. C. K. Roberts, J. Feeney, A. Gronenborn, and G. M. Clore, *Biochemistry*, 1984, **23**, 4733.
98. J. N. Champness, D. K. Stammers, and C. R. Beddell, *FEBS Lett.*, 1986, **199**, 61.
99. C. R. Groom, J. Thillet, A. C. North, R. Pictet, and A. J. Geddes, *J. Biol. Chem.*, 1991, **266**, 19890.
100. V. I. Polshakov, B. Birdsall, and J. Feeney, *Biochemistry*, 1999, **38**, 15962.
101. S. Sasso, I. Protasevich, R. Gilli, A. Makarov, and C. Briand, *J. Biomol. Struct. Dyn.*, 1995, **12**, 1023.
102. S. P. Sasso, R. M. Gilli, J. C. Sari, O. S. Rimet, and C. M. Briand, *Biochim. Biophys. Acta*, 1994, **1207**, 74.
103. J. M. Johnson, E. M. Meiering, J. E. Wright, J. Pardo, A. Rosowsky, and G. Wagner, *Biochemistry*, 1997, **36**, 4399.
104. G. Martorell, M. J. Gradwell, B. Birdsall, C. J. Bauer, T. A. Frenkel, H. T. Cheung, V. I. Polshakov, L. Kuyper, and J. Feeney, *Biochemistry*, 1994, **33**, 12416.
105. S. B. Shuker, P. J. Hajduk, R. P. Meadows, and S. W. Fesik, *Science*, 1996, **274**, 1531.
106. P. J. Hajduk, R. P. Meadows, and S. W. Fesik, *Science*, 1997, **278**, 497.
107. P. J. Hajduk, S. Boyd, D. Nettesheim, V. Nienaber, J. Severin, R. Smith, D. Davidson, T. Rockway, and S. W. Fesik, *J. Med. Chem.*, 2000, **43**, 3862.
108. P. J. Hajduk, J. Dinges, J. M. Schkeryantz, D. Janowick, M. Kaminski, M. Tufano, D. J. Augeri, A. Petros, V. Nienaber, P. Zhong, R. Hammond, M. Coen, B. Beutel, L. Katz, and S. W. Fesik, *J. Med. Chem.*, 1999, **42**, 3852.
109. P. J. Hajduk, J. Dinges, G. F. Miknis, M. Merlock, T. Middleton, D. J. Kempf, D. A. Egan, K. A. Walter, T. S. Robins, S. B. Shuker, T. F. Holzman, and S. W. Fesik, *J. Med. Chem.*, 1997, **40**, 3144.

Received March 15, 2001